# Studies on N1-Methyladenosine Modification of rRNA in Multicellular Organisms

# Studies on $N^1$-Methyladenosine Modification of rRNA in Multicellular Organisms

January 2018

Wataru YOKOYAMA

# Studies on $N^1$-Methyladenosine Modification of rRNA in Multicellular Organisms

A Dissertation Submitted to

the Graduate School of Life and Environmental Sciences,

the University of Tsukuba

in Partial Fulfillment of the Requirements

for the Degree of Doctor of Philosophy in Biotechnology

(Doctoral Program in Life Sciences and Bioengineering)

Wataru YOKOYAMA

# Contents

# Chapter I.

## Preface

Genetic information is transferred from DNA into proteins. This biological phenomenon is termed 'Central Dogma'. Its flow can be divided into DNA replication, transcription, and translation. RNAs play pivotal roles in the transcription and translation steps. For example, DNA is transcribed into messenger RNA (mRNA) and this mRNA is translated by ribosomes, which are composed of ribosomal RNAs (rRNAs) and ribosomal proteins. During translation, transfer RNAs (tRNAs) bring specific amino acids to the ribosomes. The functions of these RNAs can be regulated post-transcriptionally (referred to as RNA modifications). RNA modifications are present in all kingdoms of life. Further, over 100 different types of modifications have been identified (1).

Among the known RNA modifications, the $N^1$-methyladenosine ($m^1A$) modification, which is an N1 atom methylated ribonucleotide, is well-studied. Over 50 years ago, $m^1A$ was first documented using yeast and mammalian RNAs (2). Until now, $m^1A$ modifications in tRNAs have been shown to increase its structural stability and induce correct folding (3). Additionally, enzymes catalyzing the $m^1A$ modification of tRNA have been identified not only in yeast but also in mammals (4, 5). On the other

hand, the methyltransferase(s) and physiological functions of the rRNA $m^1A$ modification, especially in multicellular organisms, are poorly understood.

Recently, Peifer *et al.* have reported that yeast rRNA processing protein 8 (Rrp8) is responsible for the $m^1A$ modification of yeast 25S rRNA (6). Therefore, in chapter II, I focused on the mammalian homolog of yeast Rrp8, nucleomethylin (NML), and investigated its involvement in the rRNA $m^1A$ modification using mammalian cells. I showed that NML is required for the $m^1A$ modification in human and mouse 28S rRNA, and contributes to formation of the 60S ribosomal subunit. Furthermore, I demonstrated that NML regulates the cell growth via a p53-dependent mechanism.

*Caenorhabditis elegans* (*C. elegans*) is a frequently used model organism for various biological studies, such as development, behavior, and aging (7, 8). Hence, in chapter III, to reveal the physiological significance of the rRNA $m^1A$ modification *in vivo*, I investigated the function of T07A9.8, a *C. elegans* homolog of human NML. The results demonstrated that T07A9.8 is involved in the regulation of autophagy and lifespan. Notably, it has been considered that autophagy plays a key role in longevity (9-12). Collectively, these novel discoveries suggest the proposition that the rRNA $m^1A$ modification links autophagy to the regulation of lifespan in multicellular organisms.

## Chapter II.

# Mammalian NML-mediated $m^1A$ modification of rRNA links ribosomal subunit formation to cell proliferation in a p53-dependent manner


## Abstract

Ribosomal RNAs (rRNAs) act as scaffolds and ribozymes in ribosomes, and these functions are modulated by various post-transcriptional modifications. However, the biological roles of base methylation, a well-conserved modification of rRNAs, are largely unknown.

In this study, using human and mouse cells, I demonstrated that a nucleolar protein, nucleomethylin (NML; also known as RRP8), is required for the $N^1$-methyladenosine ($m^1A$) modification of 28S rRNA. Furthermore, NML contributes to the 60S ribosomal subunit formation. Intriguingly, NML depletion increases ribosomal protein L11 (RPL11) levels in the ribosome-free fraction. This increment upregulates the p53 protein levels through an RPL11-MDM2 complex, and thereby activates the p53 pathway. In consequence, the growth of NML-depleted cells is suppressed in a p53-dependent manner.

These findings reveal a novel biological function of the rRNA $m^1A$ modification, which links ribosomal subunit formation to p53-mediated inhibition of cell proliferation in mammalian cells.

## Introduction

Ribosomal RNAs (rRNAs) function as scaffolds for ribosomal proteins and ribozymes for peptide bond formation (13, 14). Biosynthesis of rRNA comprises transcriptional and post-transcriptional modification of precursor (pre)-rRNAs as well as the processing of pre-rRNAs into mature 28S, 18S and 5.8S rRNAs (15). Nucleotide modifications of rRNA regulate the function and stability of ribosomes (16). There are three main types of chemical modifications of rRNA – conversion of uridine to pseudouridine (pseudouridylation); methylation of 2′-hydroxyls (2′-*O*-ribose methylation); and alteration of bases, most of which undergo methylation at its different positions (base methylation) (16). Of these modifications, base methylations are the most conserved in terms of their total number and position among living organisms, and are commonly found at approximately ten positions in eukaryotic rRNAs (17, 18). Base methylation is considered to expand the structural repertoire of RNA through facilitating base stacking by increasing hydrophobicity and adjusting steric hindrance (19). To date, base methylation of rRNA and the genes responsible for it (*Bud23*, *Rrp8*, *Nop2*, *Rcm1*, *Bmt2*, *Bmt5* and *Bmt6*) have been identified in budding yeast (6, 20-22). The recent report has shown that yeast and worm homologs of human NSUN5 methylate C2278 of *Saccharomyces cerevisiae* 25S rRNA and C2381 of *Caenorhabditis elegans* 26S rRNA.

In addition, the reduction in the levels of NSUN5 homologs decreases translational fidelity in yeast and increases the lifespan of *S. cerevisiae*, *C. elegans* and *Drosophila melanogaster* (23). Until now, the human homolog of yeast Bud23, WBSCR22 (Merm1), has been shown to mediate $N^7$-methylation of G1639 of 18S rRNA and contribute to its maturation in cells (24). However, little is known about the base methyltransferase of 28S rRNA in mammals.

In all organisms, ribosomes serve as the sole site of protein synthesis, and their biogenesis is strictly regulated. The mammalian ribosomes comprise two subunits composed of rRNAs and ribosomal proteins (25, 26). The small subunit (40S) is formed from a single molecule of rRNA (18S rRNA) and 33 ribosomal proteins (ribosomal proteins of the small ribosomal subunit; RPSs). Conversely, the large subunit (60S) contains three rRNA molecules (28S, 5.8S, and 5S rRNA) and 47 ribosomal proteins (ribosomal proteins of the large subunit; RPLs). Interestingly, the defects of ribosome biogenesis are coupled to inhibition of cell proliferation that is mediated by p53 (27-29). p53 functions as a tumor suppressor, and its activation induces cell cycle arrest and apoptosis, resulting in the suppression of cell growth (30-32). In addition to these reports, recent studies have been suggested that quantitative and qualitative changes in ribosomes are associated with numerous physiologic and pathologic events (33-37).

However, it remains unclear whether and how the base methylations of rRNAs regulate ribosomal functions and related biological events in mammals.

Nucleomethylin (NML; also known as RRP8) is a nucleolar protein that binds to dimethyl lysine at position 9 of histone H3 (H3K9me2) in cells and suppresses rRNA transcription in response to glucose deprivation (38, 39). NML contains the Rossmann-fold methyltransferase-like domain in its C-terminal half, and binds to *S*-adenosyl-L-methionine (SAM), while NML does not exhibit methyltransferase activity toward histones (39). Recently, the yeast NML homolog Rrp8 has been identified as a gene responsible for the SAM-dependent $N^1$-methyladenosine ($m^1A$) modification in the 25S rRNA (6). However, the contribution of NML to $m^1A$ modification has yet to be elucidated.

In this study, using mammalian cells, I revealed that NML is responsible for $m^1A$ modification of 28S rRNA and contributes to the formation of 60S ribosomal subunit, and that NML deficiency inhibits cell proliferation in a p53-dependent manner.

## Materials and Methods

### Cell culture

Human epithelial adenocarcinoma HeLa cells were provided by the RIKEN Catalysis Research Center through the National Bio-Resource Project of the Ministry of Education, Culture, Sports, Science and Technology, Japan. SV40 large T-antigen transformed *NML* WT and KO mouse embryonic fibroblasts (MEFs) were generated from C57BL/6J background wildtype and *NML*-KO mice, respectively (40). Human colon carcinoma HCT116 $p53^{+/+}$ and $p53^{-/-}$ cells were kindly provided by Dr. Bert Vogelstein (John Hopkins University, USA) (41). All animal experiments were approved and performed in accordance with the guidelines for the care and use of laboratory animals at University of Tsukuba. For MEF isolation, embryos at 13.5 days post-coitum from C57BL/6J mice (CLEA Japan, Japan) were used. After the removal of the head and visceral tissues, the remaining bodies were washed and dissociated. Cells were plated on dishes and incubated 37 °C with 5% $CO_2$. The next day, floating cells were removed by washing in phosphate-buffered saline (PBS). MEFs were used within three passages. All cells were maintained in Dulbecco's modified Eagle's medium (DMEM; Gibco, Thermo Fisher Scientific, USA) supplemented with 10% fetal bovine serum (FBS; Gibco, Thermo Fisher Scientific) and penicillin-streptomycin (Sigma-

Aldrich, USA).

## Antibodies

Antibodies against the following proteins and epitopes were used in my study: anti-β-actin (A5316; Sigma-Aldrich); anti-α-tubulin (T5168; Sigma-Aldrich); anti-Histone H3 (9715; Cell Signaling Technology, USA); anti-1-methyladenosine (D345-3; MBL, Japan); anti-RPL11 (14382; Cell Signaling Technology); anti-MDM2 (sc-96; Santa Cruz Biotechnology, USA); anti-p53 (DO-1; sc-126; Santa Cruz Biotechnology); anti-p21 (F-5; sc-6246; Santa Cruz Biotechnology); anti-Bax (ab7977; Abcam) and an unconjugated affinity purified isotype control immunoglobulin (IgG) from mouse (sc-2025; Santa Cruz Biotechnology). Previously reported anti-human and mouse NML antibodies were used (39, 40).

## RNA interference experiment

To generate stable knockdown cell lines, cells were transfected with the piGENE™ hU6 plasmid (iGENE Therapeutics, Japan) containing sequences targeting NML, green fluorescent protein (GFP) or luciferase (Luc). The transfected cells were selected with puromycin. The target sequences were:

5’-GCCGCTTTGAGGATGTTCGAA-3’ for shNML#1

5’-GGGTAGTACTACAAATGATCC-3’ for shNML#2

5’-GGCTACGTCCAGGAGCGCACC-3’ for shGFP

5’-GTGCGCTGCTGGTGCCAACCC-3’ for shLuc.

For transient knockdown, cells were transfected with 20 nM of Stealth RNAi™ short interfering RNA (siRNA) (Invitrogen, USA) using Lipofectamine® RNAiMAX (Invitrogen) according to the manufacturer’s protocol. The target sequences were as follows:

5’-CCGCUUUGAGGAUGUUCGAACCUUU-3’ for siNML#1 (human)

5’-CCUCAUACAUUAAGCCGCAAGCAGU-3’ for siNML#2 (human)

5’-CCAAACUCGGCUUUAAGAUUAUCUA-3’ for siNML (mouse)

5’-ACACAUCGAUCUGGGUAUCAAAUAU-3’ for siRPL11.

Stealth RNAi™ Luciferase Reporter control (siLuc) was used as a negative control.

## Plasmid construction and mutagenesis

A plasmid containing mouse wild-type NML was constructed by inserting the Hind III-Not I (blunt ended with Klenow)-digested fragment from FLAG- and HA-tagged mouse NML in pcDNA3 into the Xho I (filled with Klenow) site of the plasmid pPB-CAG.

EBNXN (kindly provided by Dr. Allan Bradley, Wellcome Trust Sanger Institute, UK). Mutations were introduced by performing site-directed mutagenesis and PCR. The primer sequences were as follows (induced mutations are underlined):

mouse NML mt1 (G317D, G319R), 5'-GCTGACTTTGACTGTAGAGATTGCCGC-3'

mouse NML mt2 (G317Q), 5'-GCTGACTTTGGCTGTGAAGATTGCCGC-3'.

## RNA immunoprecipitation (RIP)

RIP was performed as previously described (42) with minor modifications. For RIP against NML using nuclear lysates, cells were harvested and resuspended in 450 μl buffer A [10 mM HEPES (pH 7.5), 10 mM KCl, 0.1 mM EDTA] (43) and kept on ice for 15 min. Fifty microliters of buffer A including 5% Nonidet P-40 (NP-40) were added. Nuclei were pelleted by centrifugation at 800 g for 5 min at 4 °C. Then, whole cells or nuclei were suspended in 200 μl cold lysis buffer [10 mM 4-(2-hydroxyethyl)-1-piperazineethanesulfonic acid (pH 7.5), 300 mM KCl, 5 mM $MgCl_2$, 0.5% NP-40, 1 mM dithiothreitol, EDTA-free protease inhibitor cocktail (Nacalai Tesque, Japan) and 100 U/ml RNase Inhibitor (Toyobo, Japan)]. The whole-cell or nuclear extracts were centrifuged at 15,000 g for 15 min at 4 °C, and the supernatant was pre-cleared using protein G Sepharose® beads (GE Healthcare, UK) and treated with DNase I (Wako Pure

Chemical Industries, Japan) (60 U/100 μl lysate) for 30 min on ice. The samples (2-10 μg) were incubated with pre-binding antibodies (5 μg) and protein G Sepharose® beads in 1000 μl NT2 buffer [50 mM Tris-HCl (pH 7.5), 150 mM NaCl, 1 mM $MgCl_2$ and 0.05% NP-40] including 100 U of RNase inhibitor, 10 mM dithiothreitol and 20 mM EDTA overnight at 4 °C. The beads were washed twice with NT2 buffer and resuspended in 100 μl of NT2 buffer. The suspension was mixed with 100 μl of proteinase K buffer [30 μg proteinase K, 20 mM Tris-HCl (pH 7.8), 10 mM EDTA and 1% sodium dodecyl sulfate (SDS)] and incubated for 30 min at 55 °C. After centrifugation, RNAs were purified from the supernatant using phenol-chloroform-isoamyl alcohol and analyzed by performing qRT-PCR. The whole-cell or nuclear extracts were used as input samples for normalization of qRT-PCR data.

## Western blotting

For Western blotting, cells were lysed with RIPA buffer [20 mM Tris-HCl (pH7.5), 150 mM NaCl, 2 mM EDTA, 0.8% NP-40, 0.1% SDS and 0.5% sodium deoxycholate]. Cell extracts were separated by performing SDS-PAGE and transferred to a polyvinylidene difluoride membrane using transfer apparatus according to the manufacturer's protocol (Bio-Rad Laboratories, USA). The antibodies used are described in the Antibodies

section. For quantitative analyses of Western blotting data, band intensities were measured by using Multi Gauge version 3.0 software (Fujifilm, Japan). Each protein level was normalized to the protein levels of β-actin.

## qRT-PCR

To quantify rRNA or mRNA levels, aliquots of total RNA (500 ng) were reverse transcribed with a pd $(N)_6$ random primer and 250 μM of deoxy nucleoside triphosphates (dNTPs). Quantitative reverse-transcription (qRT)-PCR was performed with primers for the indicated rRNAs or genes (Table 1). The expression level of each gene in human and mouse cells was normalized to the mRNA levels of genes encoding human β-actin (*ACTB*) and mouse cyclophilin (*Ppia*), respectively.

## Detection of rRNA methylation with site-specific semi-quantitative RT-PCR

To quantify rRNA methylation levels, I performed a site-specific rRNA methylation assay based on qRT-PCR (35, 37). Total RNA was extracted and purified using Sepasol-RNA I Super G (Nacalai Tesque) according to the manufacturer's instructions. Total RNA (500 ng) were reverse transcribed using ReverTra Ace® (Toyobo) and 1 μM of

each reverse primer targeting a sequence downstream to a specific methylation site, with either a low (2.5 μM) or high (250 μM) dNTP concentration. qRT-PCR was performed with SYBR® Premix Ex Taq™ II (Takara, Japan) using a Thermal Cycler Dice™ Real-Time System (Takara). The methylation level was calculated following the function $2^{(CT^{low} - CT^{high})}$, where the CT (threshold cycle) value obtained with the qRT-PCR reaction at the low dNTP concentration was normalized to that obtained at the high dNTP concentration. The primer sequences used in this assay are listed on Table 2.

## Primer extension

Primer extension was performed as per described protocols (21, 44) with minor modifications. One micromole of DNA primer was $^{32}$P-5'-terminally labeled by incubation in a final volume of 25 μl with 15 μCi γ-[$^{32}$P]ATP and 9 U of polynucleotide kinase in protruding kinase buffer (Toyobo). The mixture was incubated at 37 °C for 1 h. The reaction mixture was then purified using Illustra™ MicroSpin™ G-25 columns (GE Healthcare). For the extension reaction, 0.5 μl of the $^{32}$P-5'-phosphorylated primer was annealed by heating for 3 min at 95 °C, followed by cooling on ice using 0.2 μg total RNA in 4.75 μl RT buffer (Toyobo) containing 2.5 μM dNTPs. Annealed primers were extended using 0.25 μl ReverTra Ace® (25 U) for 1 h at 42 °C, stopped by the

addition of 5 μl formamide loading dye and frozen at −80 °C. Primer extension products were resolved by performing electrophoresis on 8% polyacrylamide gels containing 4 M urea. Gels were dried and exposed to Amersham Hyperfilm™ ECL (GE Healthcare). The primer sequences for primer extension are listed on Table 2.

## Quantification of methylated ribonucleosides with LC-MS/MS

28S rRNA was isolated from total RNA by performing agarose gel electrophoresis and gel extraction with the NucleoSpin® Gel and PCR Clean-up system (MACHEREY-NAGEL, Germany) according to the instruction manual. After denaturation by heating at 100 °C for 3 min, 1-2 μg of 28S rRNA was chilled on ice immediately. Denatured RNA was hydrolyzed by nuclease P1 (1 U, Wako Pure Chemical Industries) in 10 mM ammonium acetate buffer (pH 5.3) at 45 °C for 2 h, subsequently dephosphorylated by incubating with phosphodiesterase I (0.0002 U, Sigma-Aldrich), alkaline phosphatase (0.3 U, Toyobo) and 0.1 volume of 1 M ammonium bicarbonate buffer (pH 7.9) at 37 °C for 2 h, as described previously (45). Ten pmol of br$^5$U (Tokyo Chemical Industry, Japan) were added into the mixture as an internal standard. The enzymes were subsequently removed by acetone precipitation. The supernatant was evaporated, and the ribonucleoside pellet was dissolved with 15 μl of HPLC-grade water (Wako Pure

Chemical Industries).

Individual ribonucleosides were quantified using a Shimadzu Nexera™ UHPLC system coupled to LCMS-8050™ triple quadrupole mass spectrometer (Shimadzu, Japan). Reverse-phase HPLC separation was carried out using a Kinetex™ 2.6 μm C18 column (2.1×150 mm, Phenomenex, USA) with a VANGUARD™ Pre-Column (2.1×5 mm, Waters, USA) at 30 °C with 0.1% formic acid in 80% acetonitrile (solvent B) gradient in 0.1% formic acid (solvent A) at a flow rate of 0.2 ml/min. The water-dissolved sample (5 μl) was injected and eluted with the following gradient elution: initial isocratic elution with 0% solvent B for 3 min, followed by linear gradient elution from 0 to 8% B until 19 min, jumping to 100% B within 2 min and holding the status until 25.5 min. The column was then subsequently returned to the start conditions within 1 min and equilibrated for 4.5 min before the next sample injection. For determining elution positions of ribonucleosides on the chromatogram, standard chemicals of $m^1A$ (Santa Cruz Biotechnology), $N^6$-methyladenosine ($m^6A$) (Carbosynth, UK), and $br^5U$ were used, and their retention times were revealed as 2.23 min, 15.1 min and 11.58 min, respectively.

The mass spectrometer was operated with an ion-spray source at 300 °C in positive ion mode, with unit resolution for Q1 and Q3, and other optimized parameters: interface

voltage, 4.0 kV; interface current, 0.1 μA; flow rate of nebulizer gas, 3 l/min; flow rate of heating gas, 10 l/min; flow rate of drying gas, 10 l/min; collision gas (Ar), 270 kPa; desolvation line temperature, 250 °C; heat block temperature, 400 °C; conversion dynode potential, 10 kV; detector potential, 2.44 kV. Multiple reaction monitoring was used for detection of nucleosides with a dwell time of up to 100 ms. Q1 was set to transmit the parental ions $MH^+$ at m/z 282.1, 282.1 and 324.6 for $m^1A$, $m^6A$, and $br^5U$, respectively. The daughter ions were monitored in Q3 at m/z 150.1, 150.1, and 193.05 for $m^1A$, $m^6A$, and $br^5U$, respectively. Linear calibration curves were obtained daily. All of the solvents and reagents used in this analysis were HPLC grade. The control of instrument and data analyses were performed using the LabSolutions LCMS (Ver.5.60) software (Shimadzu).

## $m^1A$-RIP

For RIP against $m^1A$ containing RNA, total RNAs were extracted using Sepasol-RNA I Super G and treated with DNase I. Purified RNAs were fragmented using an NEBNext® Magnesium RNA Fragmentation Module (New England Biolabs, USA). After adding 20 μg of glycogen, fragmented RNAs were precipitated with ethanol and resuspended in 100 μl of IPP buffer [10 mM Tris-HCl (pH 7.5), 150 mM NaCl and 0.1% NP-40]. RNA

samples were added to 100 μl of an antibody mixture that included IPP buffer and 50 μl of Protein G Sepharose® beads (50% slurry). The mixture was rotated overnight at 4 °C. The beads were washed twice with IPP buffer. Immunoprecipitated RNAs were purified by phenol‐chloroform-isoamyl alcohol extraction, and analyzed by qRT-PCR. Total RNAs were used as input samples for normalization of qRT-PCR data.

## rRNA processing

Cells were cultured with methionine-free medium for 1 h, and then with methionine-free medium containing 20 μCi/ml $^{32}$P-labeled inorganic phosphate for 1 h (28). The metabolic labeling media were removed, and the cells were cultured with normal medium for 3 h. After cell harvesting, RNA was extracted using a FastPure™ RNA Kit (Takara) and analyzed by glyoxal agarose gel electrophoresis. Total RNA was visualized by ethidium bromide staining.

## Bimolecular fluorescence complementation

The BiFC assay was performed as described previously (46). To generate plasmids expressing BiFC-tagged ribosomal proteins, the sequences of *RPS18* and *RPL11* were PCR-amplified from the cDNA of HeLa cells using primers tagged with SacI and XbaI

or ApaI and KpnI, respectively. The *RPS18* and *RPL11* segments were cloned into pBiFC-VN173 (22010, Addgene, USA) and pBiFC-VC155 (22011, Addgene), respectively (47). Using Lipofectamine® LTX (Invitrogen), these BiFC plasmids were co-transfected with a pmCherry-N1 plasmid (Clontech Laboratories, USA), which was used as an internal control. Twenty-four hours after transfection, cells were further cultured with or without 100 μg/ml puromycin for 24 h. The cells were washed twice with STM buffer [PBS with 2% FBS] and resuspended in 500 μl of STM buffer. The fluorescence intensities of Venus and mCherry were measured by a BD FACSAria™ II (BD Biosciences, USA). The BiFC signal emitted by a cell was calculated using the following function: (fluorescent intensity of Venus)/(fluorescent intensity of mCherry), following the previous method (48).

## Sucrose density gradient centrifugation

Sucrose density gradient centrifugation was performed as previous described manner (6, 49). Briefly, to investigate ribosomal subunit formation, cells were treated with 100 μg/ml cycloheximide (CHX) for 5 min at 37 °C. The cells were washed twice with PBS containing CHX (100 μg/ml) and lysed with lysis buffer [15 mM Tris-HCl (pH 7.5), 300 mM NaCl, 25 mM EDTA, 1% Triton X-100, 0.5 mg/ml heparin, 100 μg/ml CHX,

1× EDTA-free protease inhibitor cocktail (Nacalai Tesque) and 100 U/ml RNase inhibitor (Toyobo)]. The lysate was centrifuged at 9300 g for 10 min at 4 °C and loaded onto a linear 20-50% sucrose gradient buffer in 15 mM Tris-HCl (pH 8.0), 25 mM EDTA, and 300 mM NaCl. Centrifugation was conducted at 40,000 rpm for 2 h at 4 °C with a SW-41 Ti rotor (Beckman Coulter, USA), and fractions were collected from the top of the gradient (#1 to #18). The 18S and 28S rRNA levels in the fractions #1 to #18 were quantified by conducting qRT-PCR and normalized against those rRNA levels in an input RNA extracted from cells. The ratio of 18S rRNA : 28S rRNA (18S rRNA divided by 28S rRNA) was calculated as the small : large ribosomal subunit ratio.

To obtain the ribosomal or ribosome-free fractions, I performed sucrose density gradient centrifugation using lysis and gradient buffers containing 15 mM $MgCl_2$ instead of 25 mM EDTA. 18S and 28S rRNAs, and β-actin proteins were used as indicators for the ribosomal and ribosome-free fractions, respectively (50, 51).

## Analysis of protein synthesis with $^{35}$S-methionine

The quantification of protein synthesis rate was performed as previously described (52, 53). Cells were plated onto 12-well plates in complete medium, and in the case of HCT116 cells, siRNAs were transfected. One day after cell seeding or 3 days after

transfection, the culture medium was switched to methionine-free DMEM with or without 50 μg/ml CHX for 30 min at 37 °C, and cells were incubated with the same medium containing 20 μCi/ml $^{35}$S-methionine (PerkinElmer, USA) for 2 h at 37 °C. Cells were then washed twice with ice-cold PBS and solubilized in 50 μl of RIPA buffer containing protease inhibitors. The supernatant was analyzed using a liquid scintillation counter (Beckman Coulter) and obtained values were normalized against the total protein content.

## Co-immunoprecipitation

Cells were lysed in RIPA buffer supplemented with EDTA-free protease inhibitor cocktail. The same amounts of protein lysates were resuspended in TNE buffer [10 mM Tris-HCl (pH7.5), 150 mM NaCl, 1 mM EDTA, 1% NP-40] supplemented with EDTA-free protease inhibitor cocktail, and were immunoprecipitated with the indicated antibodies (1.8 μg/ml) and Dynabeads® Protein G (Invitrogen). Bound proteins were then analyzed by Western blotting.

## Cell cycle analysis by 5-ethynyl-2'-deoxturidibe staining

For 5-ethynyl-2'-deoxyuridine (EdU) staining, cells were plated ($1\times10^5$ cells/well in a

6-well plate) and cultured for 3 days after siRNA transfection. Then, cell cycle evaluation was conducted using a Click-iT® EdU Imaging Kit (Invitrogen), according to the manufacturer's protocol. First, cells were labeled with 10 μM EdU (Invitrogen) in culture medium for 1 h at 37 °C. For subsequent DNA staining, EdU-stained cells were incubated with 2 μg/ml Hoechst 33342 (Sigma-Aldrich) for 10 min. After the staining, cells were washed with PBS and subjected to FACS by using a BD FACSAria™ II instrument.

## Terminal deoxynucleotidyl transferase dUTP-biotin nick labelling assay

Cells were plated onto poly-D-lysine coated 8-well chamber slides (BD Biosciences) ($1.6\times10^4$-$2.4\times10^4$ cells/well) and cultured for 3 days after siRNA transfection. Then, the cells were fixed with 4% paraformaldehyde in PBS for 25 min at 4 °C, and in situ detection of apoptotic cells was performed using DeadEnd™ Fluorometric TUNEL System (Promega, USA), according to the manufacturer's instructions. The nuclei were then counterstained using 2 μg/ml Hoechst 33342. The cells were observed using the fluorescent microscope imaging system BIOREVO BZ-9000 (Keyence, Japan), and TUNEL-positive cells were measured in three fields per sample. The percentage of

TUNEL-positive cells was calculated as follows: (TUNEL-positive/total cells) × 100.

## Cell proliferation assay

To analyze the cell proliferation rate, cells were seeded ($1\times10^5$ cells/well) in 6-well plates and transfected them with the indicated siRNA. The cells were then trypsinized into single-cell suspensions and automatically counted using a TC10™ Automated Cell Counter (Bio-Rad Laboratories) on days 1, 2, 3, and 4, where the first day after seeding was day 0.

## Statistical analysis

The unpaired Student's *t*-test was used to compare two groups, and one-way ANOVA followed by Tukey's post-hoc test was used to compare multiple groups. The statistical analysis of fold-change data was performed by bootstrap and permutation tests using the web application BootstRatio (54).

## Results

### NML binds to 28S rRNA

A large number of RNA methyltransferases interact with the specific target RNA through their substrate-binding site (55). To date, Yang *et al*. have shown the interaction of NML with rRNAs using human non-small lung carcinoma H1299 cells (56). To confirm the interaction between NML and 28S rRNA in human epithelial adenocarcinoma HeLa cells, I performed RNA immunoprecipitation (RIP) experiments using an antibody against NML. In this assay, endogenous NML proteins were precipitated using an antibody against NML. After immunoprecipitation, RNAs were then purified from the precipitates, and 28S rRNA levels were quantified by performing quantitative reverse-transcriptase (qRT)-PCR using a specific primer set (Table 1). 28S rRNA was co-immunoprecipitated with NML from the whole cell (Fig. II-1A). Furthermore, I isolated the nuclear extracts from the cells, and detected the interaction between 28S rRNA and NML (Fig. II-1B). On the other hand, 5S rRNA was not significantly co-immunoprecipitated with NML (Fig. II-1A, B). From these results, I confirmed that NML has the potential to associate with 28S rRNA.

## NML is required for methylation of 28S rRNA

In yeast 25S rRNA, two sites with the $m^1A$ modification have been identified (6, 21), and these adenosine molecules and also the neighboring sequences are well conserved among eukaryotes, including humans and mice (Fig. II-2A; A645 and A2142 of 25S rRNA in *Saccharomyces cerevisiae* correspond to A1309 and A3625 of 28S rRNA in *Homo sapiens*, and A1136 and A3301 of 28S rRNA in *Mus musculus*, respectively). Therefore, to investigate the effect of NML on rRNA methylation, I performed site-specific semi-quantitative RT-PCR analysis (Fig. II-2B). I used HeLa cells stably expressing NML-knockdown (KD) constructs (shNML#1 and #2) (Fig. II-2C). Methylation levels around A1309, which is methylated by Rrp8 in yeast (6), were significantly lower in shNML-transfected cells than in control cells expressing shRNAs against green fluorescent protein (shGFP) (Fig. II-2D; left). In contrast, methylation levels around A3625, which is methylated by Bmt2 in yeast (21), were very low in control cells [rRNA methylation levels around A1309 and A3625 (mean ± S.D.) were 19.05 ± 0.47 and 1.32 ± 0.21, respectively.]. In addition, the methylation levels were not markedly changed by knockdown of NML (Fig. II-2D; right). Consistently, methylation levels around A1136, which corresponds to A1309 of 28S rRNA in humans, were reduced in *NML*-knockout (*NML* KO) immortalized mouse embryonic fibroblasts

(MEFs) compared with in *NML* wild-type (*NML* WT) MEFs (Fig. II-2E, F; left). Furthermore, methylation levels around A3301 were quite low and were not affected by NML depletion (Fig. II-2F; right).

Next, to determine the precise methylation site, I performed primer extension analysis. Strong stop signals at positions A1309 and A1136 were observed in 28S rRNAs of shGFP and *NML* WT cells (Fig. II-2G). By contrast, these stop signals were reduced in 28S rRNAs of NML KD and KO cells. Moreover, the reduction of methylation levels around A1136 was attenuated by the expression of FLAG- and hemagglutinin (HA) (FLAG-HA)-tagged NML, but not by the expression of control EGFP (Fig. II-2H, I). These results indicate that NML is responsible for the methylation at A1309 and A1136 in 28S rRNA of human and mouse cells.

## Rossmann-fold methyltransferase-like domain of NML is essential for 28S rRNA methylation

A previous study has revealed that the C-terminal region of NML contains a Rossmann-fold methyltransferase-like domain, which interacts with the methyl donor SAM (39) (Fig. II-3A). To investigate whether this domain is indispensable for 28S rRNA methylation induced by NML, I performed site-specific semi-quantitative RT-PCR

analysis using the immortalized MEFs, which were stably expressed FLAG-HA-tagged wild-type NML (NML-wt) or mutated NML constructs (NML-mt1 or NML-mt2). These mutated NML proteins lack the SAM-binding ability (39) (Fig. II-3A, B). Expression of NML-wt increased rRNA methylation levels around A1136 in *NML* KO MEFs (Fig. II-3C). Conversely, no significant enhancement of rRNA methylation was induced by expression of control EGFP, NML-mt1 or NML-mt2 in *NML* KO MEFs. These results suggest that NML regulates the methylation of 28S rRNA through its methyltransferase-like domain-dependent mechanism.

## NML is responsible for $m^1A$ modification of 28S rRNA

To investigate whether the NML-mediated 28S rRNA methylation is $m^1A$ modification or not, I quantified the base modifications, included in a 28S rRNA fragment by liquid chromatography/tandem mass spectrometry (LC-MS/MS). In NML KD and KO cells, the peaks corresponding to $m^1A$ were reduced compared with those in control KD and *NML* WT cells (Fig. II-4A, B). Moreover, RIP experiments using an antibody against $m^1A$ revealed that $m^1A$ modifications around A1309 and A1136 were significantly reduced by NML depletion (Fig. II-4C, D). From these results, I revealed that NML is a responsible factor for $m^1A$ modifications at positions 1309 and 1136 in human and

mouse 28S rRNA.

## NML hardly alters rRNA transcription and processing under high glucose environments

Previous reports have shown that NML inhibits rRNA transcription in human cells under glucose deprivation (39). Moreover, it has been reported that the depletion of certain factors involved in ribosome biogenesis inhibits rRNA transcription and/or processing (57). To evaluate the effect of NML KD on rRNA transcription and processing under conditions with 4.5 g/l glucose used in this study, I checked pre- and mature rRNA levels. In shNML-expressing HeLa cells, pre- and mature rRNA levels were unchanged in comparison with those in control cells (Fig. II-5A). Furthermore, the analysis of pre-rRNA processing using metabolic labeling with $^{32}$P-orthophosphate showed that there was not substantial change in the distribution patterns on gels of pre-rRNAs (47S and 45S, and 32S) and mature rRNAs (28S and 18S) between shGFP- and shNML-expressing HeLa cells (Fig. II-5B). These results indicate that NML modulates rRNA base methylation without altering rRNA transcription and processing under high glucose conditions.

## NML participates in the ribosomal subunit association

Modifications of rRNA contribute to the ribosomal subunit formation and association (16, 58-60). To investigate the effect of NML reduction on the interaction between ribosomal subunits, I conducted bimolecular fluorescence complementation (BiFC) to visualize ribosomal subunit joining (46). The 40S ribosomal protein S18 (RPS18) and 60S ribosomal protein L11 (RPL11), which are positionally adjacent to each other on the surface of each subunit, were tagged with the N- or C-terminal halves of the yellow fluorescent protein Venus, respectively (yielding S18-VN and L11-VC; Fig. II-6A). Subunit interaction was detected as Venus signal (hereafter referred to as BiFC signal). I quantified the BiFC signal using fluorescence activated cell sorting (FACS) and confirmed that the signal was only detected from the S18-VN and L11-VC co-transfected cells (Fig. II-6B; S18-VN/L11-VC). Moreover, the BiFC signal was dramatically reduced when cells were treated with puromycin, an aminoacyl-tRNA-like molecule which induces 80S ribosome dissociation (46, 61) (Fig. II-6B-D). These results support that the BiFC signal derived from S18-VN and L11-VC expression is a consequence of subunit interaction. Knockdown of NML increased the population of cells, emitted a low BiFC signal, and decreased the proportion of cells that emitted a high BiFC signal (Fig. II-6C). Consistently, the median of BiFC signals was also

decreased by NML KD (Fig. II-6D).

## NML contributes to the 60S ribosomal subunit formation without changing the protein production rate

To evaluate the ribosomal subunit formation, I performed sucrose density gradient centrifugation under the EDTA existent conditions, which induce the dissociation of the 80S ribosome complexes into the 40S and 60S subunits (6). In this experiment, the cell lysates were centrifuged and fractionated, and the ribosomal subunit ratio was quantified by measuring the 18S and 28S rRNA levels in each fraction (Fig. II-7A). The ratio of 18S rRNA : 28S rRNA (amount of 18S rRNA was divided by that of 28S rRNA) in shNML cells was significantly higher than that of shGFP cells (Fig. II-7B). Notably, in these cell lines, 18S and 28S rRNAs were distributed to similar extents in fractions 4-8 and 9-15, respectively (Fig. II-7A). Considering that this assay separates cellular organelles including ribosomal subunits, depending on their individual densities (mass/volume), these results indicate that NML reduction results in fewer 60S subunits, rather than the formation of abnormal subunits.

The primary function of ribosome is protein synthesis. Hence, to investigate whether NML depletion alters bulk protein translation, I measured the incorporation of

$^{35}$S-labeled methionine ($^{35}$S-Met) into polypeptide chains. Pretreatment with protein synthesis inhibitor cycloheximide (CHX) substantially blocked amino acid incorporation (Fig. II-7C). In NML KD cells, the rates of $^{35}$S-Met incorporation were not markedly different from those in control cells. Overall, these results suggest that NML is involved in the formation of 60S ribosomal subunits without affecting bulk protein synthesis.

## NML depletion induces the p53 protein accumulation through RPL11

Abundance of ribosomal proteins outside of the ribosome increases when ribosomal biogenesis is perturbed by nucleolar stress (62-64). Several ribosomal proteins, including RPL11, bind to MDM2 and inhibit the E3 ubiquitin ligase function of MDM2 toward p53, leading to p53 accumulation and activation (65-67). To investigate whether NML is involved in the regulation of p53 activity through ribosomal proteins, I analyzed the levels of RPL11 protein in the ribosome-free fraction by performing sucrose density gradient centrifugation under the EDTA absent conditions followed by Western blotting. The amount of ribosome-free RPL11 was increased in shNML cells (Fig. II-8A), indicating the enhanced RPL11 accumulation outside of the ribosome. Furthermore, co-immunoprecipitation experiments showed that the interaction between

RPL11 and MDM2 was increased in shNML cells (Fig. II-8B). Considering that p53 activity in the HeLa cells and immortalized MEFs is inhibited by E6 protein from oncogenic HPV type 16 and by SV40 large T-antigen, respectively (68, 69), these cells are not suitable for the analysis of p53 functions. Thus, I used human colon carcinoma HCT116 *p53* wild-type ($p53^{+/+}$) and null ($p53^{-/-}$) cells, and investigated the possibility that NML depletion induces p53 activation through RPL11. In $p53^{+/+}$ cells, NML KD increased p53 protein levels, and this p53 accumulation was abrogated by the concomitant reduction of RPL11 (Fig. II-8C).

## NML depletion activates the p53 pathway

Next, I evaluated the expression of p53 target genes. NML KD upregulated the p53 target gene expression at both the mRNA and protein levels in $p53^{+/+}$ cells, but not in $p53^{-/-}$ cells (Fig. II-9A, B). Additionally, the increment in the p53 target genes induced by NML depletion was also observed in normal MEFs, but not in the immortalized MEFs (Fig. II-9C). Taken together, these results indicate that NML deficiency increases the RPL11-MDM2 interaction and induces the activation of p53 pathway.

## NML reduction induces cell cycle arrest and apoptosis, and inhibits translation through the p53 pathway.

p53 contributes to the regulation of cell proliferation by inducing cell cycle arrest and apoptosis, or by inhibiting protein synthesis (30-32, 70). Therefore, I investigated the effect of NML on these p53-dependent cellular events. Firstly, I performed cell cycle analysis, and observed that NML KD decreased the proportion of S-phase cells and increased the ratio of G2- and M- (G2/M) phase cells in a p53-dependent manner (Fig. II-10A). Moreover, a terminal deoxynucleotidyl transferase-mediated dUTP-biotin nick end labeling (TUNEL) assay showed that the percentage of TUNEL-positive cells was significantly increased by NML KD in $p53^{+/+}$ cells, while this was not the case in $p53^{-/-}$ cells (Fig. II-10B). Further, the rates of $^{35}$S-Met incorporation into synthesized proteins were reduced by NML KD in $p53^{+/+}$ cells (Fig. II-10C). On the other hand, in $p53^{-/-}$ cells, the rates of the labeled amino acid incorporation were not significantly changed by NML reduction.

## NML regulates cell proliferation in a p53-dependent manner

Finally, I assessed the influence of NML depletion on cell proliferation, and revealed that NML KD suppressed cell growth in a p53-dependent manner (Fig. II-11A).

Additionally, in both HCT116 *p53*$^{+/+}$ and *p53*$^{-/-}$ cells, NML KD also significantly reduced methylation levels around A1309, as well as interactions between ribosomal subunits (Fig. II-11B, C). Altogether, these findings suggest that NML modulates the large ribosomal subunit formation through $m^1A$ modification of 28S rRNA, thereby regulating cell proliferation via the p53-dependent mechanisms.

## Discussion

In this chapter, I showed that the nucleolar protein NML regulates $m^1A$ modification of 28S rRNA through a SAM-binding domain-dependent mechanism (Fig. II-1-4). Additionally, NML depletion decreases 60S ribosomal subunit formation (Fig. II-7). Intriguingly, I observed that NML depletion induces RPL11-MDM2 interactions and increases the levels of p53 protein, thereby activating the p53 pathway (Fig. II-8, 9). Consequently, the proliferation of NML-depleted cells is suppressed via p53-dependent cell cycle arrest, apoptosis, and protein synthesis inhibition (Fig. II-10, 11). Therefore, these results suggest that NML is required for the $m^1A$ modification of 28S rRNA, and that NML deficiency inhibits cell proliferation in a p53-dependent manner.

NML was originally identified as an H3K9me2-binding protein that forms a complex with SIRT1 and SUV39H1 to suppress rRNA transcription under glucose starvation (39). My data raise the question of how the molecular function of NML switches from an epigenetic suppressor for rRNA transcription to a base methyltransferase of rRNA. Interestingly, some recent reports have shown that NML binds to rRNA and also several ribosomal proteins under normal glucose conditions (56, 71). Conversely, the interaction between NML and rRNA is disturbed after glucose deprivation, thereby the recruitment of SIRT1 to NML is enhanced. Indeed, I confirmed

that NML interacts with 28S rRNA in HeLa cells (Fig. II-1) and that NML depletion does not change the levels of rRNA transcription at a 4.5 g/l glucose concentration (Fig. II-5). These results raise the possibility that NML bifunctionally regulates the distinct steps of ribosome biogenesis, involving rRNA transcription and methylation, in response to environmental changes.

Of the rRNA modifications, 2'-*O*-ribose methylation, which affects not only ribosome biogenesis but also ribosomal functions, including translational efficiency and fidelity (16), is one of the best characterized modifications. Furthermore, Fibrillarin (FBL) has been identified as a 2'-*O*-ribose methyltransferase (42, 72). Recently, it has been reported that p53 directly represses *FBL* gene transcription and decreases the 2'-*O*-ribose methylation of rRNAs, and these changes induce the impairment of translational function of ribosomes, such as the stop-codon readthrough and amino acid misincorporation (37). Furthermore, FBL overexpression facilitates tumorigenesis and is correlated to poor survival of cancer-affected individuals (73-75). These observations imply that rRNA modification plays a crucial role in cancer development. Intriguingly, the levels of $m^1A$-modified nucleosides are elevated in the urine of individuals with cancer (76, 77). Hence, my results suggest that the NML-dependent $m^1A$ modification of rRNA could influence cancer development through the p53 pathway. As a further

study, the potential roles of NML-mediated rRNA modifications in cancer development should be explored.

# Fig. II-1

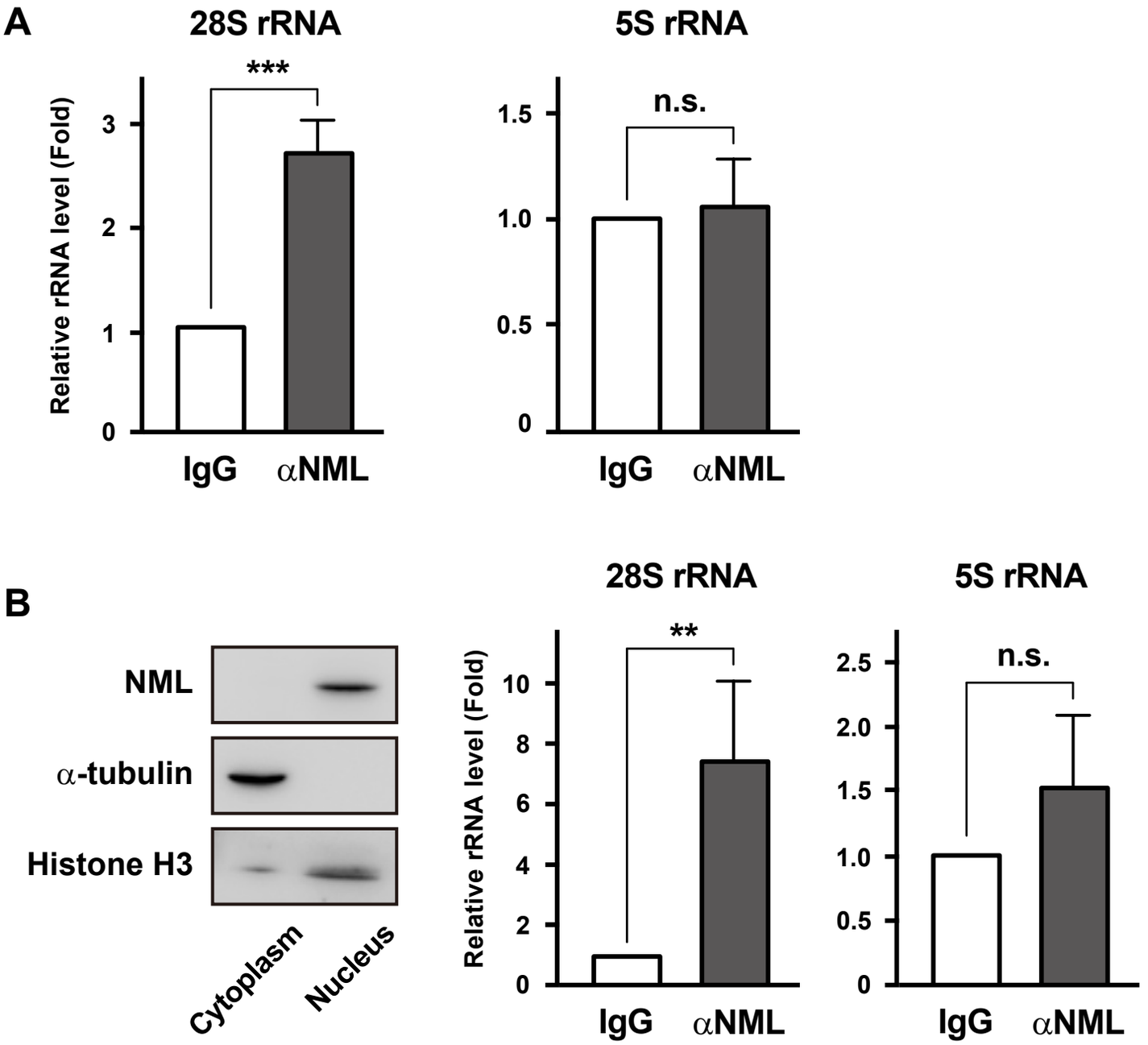


**Fig. II-1 NML binds to 28S rRNA.**

**(A, B)** Interaction between rRNA and NML in whole-cell extracts (A) and nuclear extracts (B) of HeLa cells. The binding of NML to 28S or 5S rRNAs was examined with RIP assay using an anti-NML antibody (αNML). An conjugated affinity purified immunoglobulin (IgG) from mouse was used as a control. In the left panel in B, protein levels of NML in the cytoplasmic or nuclear fractions were determined by Western blotting. α-tubulin and histone H3 were used as each fraction marker. Mean values ± S.D. are shown (n = 3). ***P* < 0.01; ****P* < 0.005; n.s., not significant (bootstrap and permutation tests).

# Fig. II-2

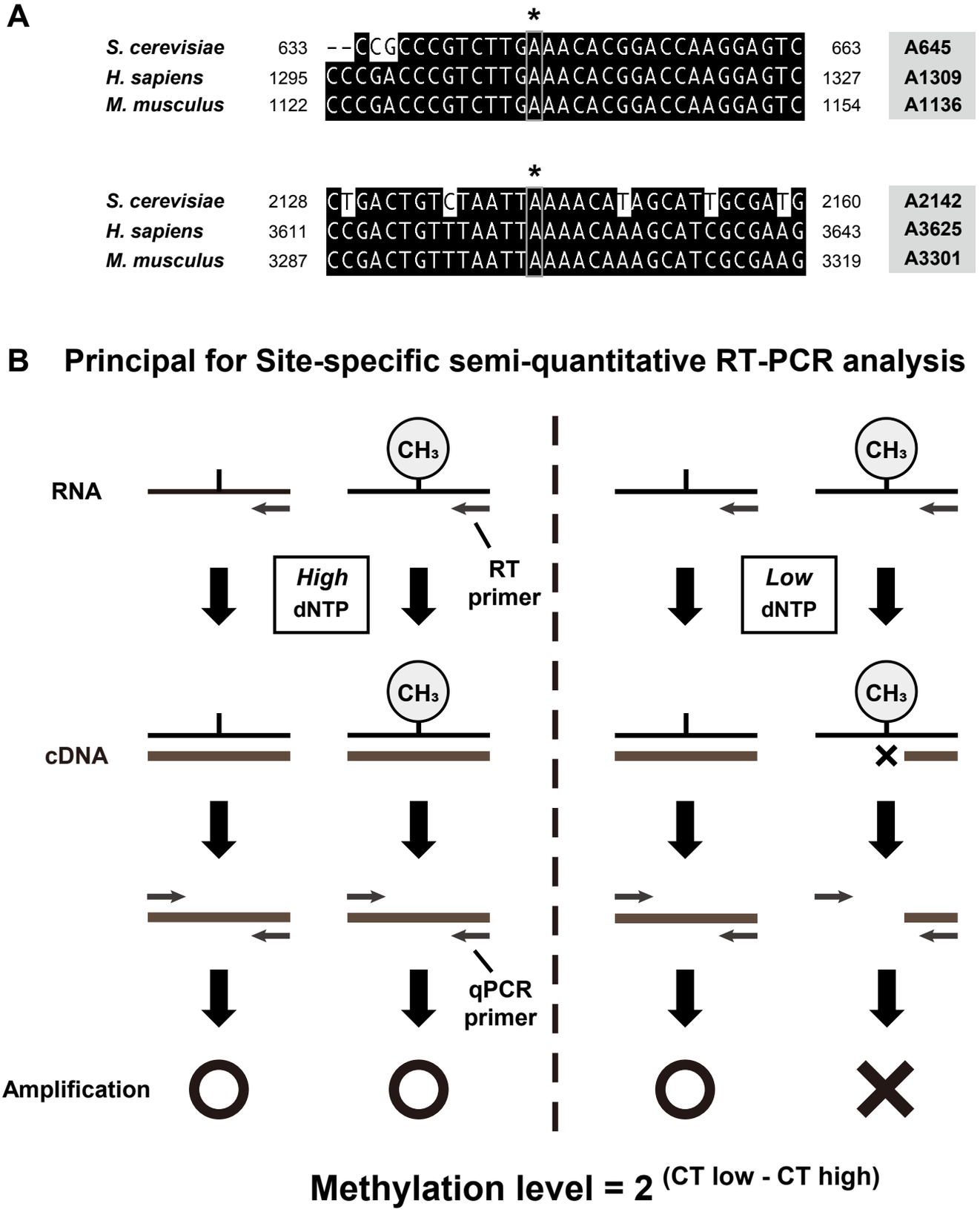


**Fig. II-2 NML is need for methylation of 28S rRNA.**

**(A)** Multiple sequence alignment of the regions neighboring two sites of m¹A (A645 and A2142 in squares) of 25S rRNA (633-663 and 2128-2160) in *S. cereviaiae*, of 28S rRNA (1295-1327 and 3611-3643) in *H. sapiens* and of 28S rRNA (1122-1154 and 3287-3319) in *M. musculus* are shown. Conserved adenosine ribonucleotides focused in this study are marked with asterisks (*).

**(B)** Schematic representation of the site-specific semi-quantiitative RT-PCR analysis for RNA methylation detection. The primers used for reverse transcription and qPCR are indicated as the gray arrows.

(***Figures and Figure legends continued on next page***)

# Fig. II-2 (*continued*)

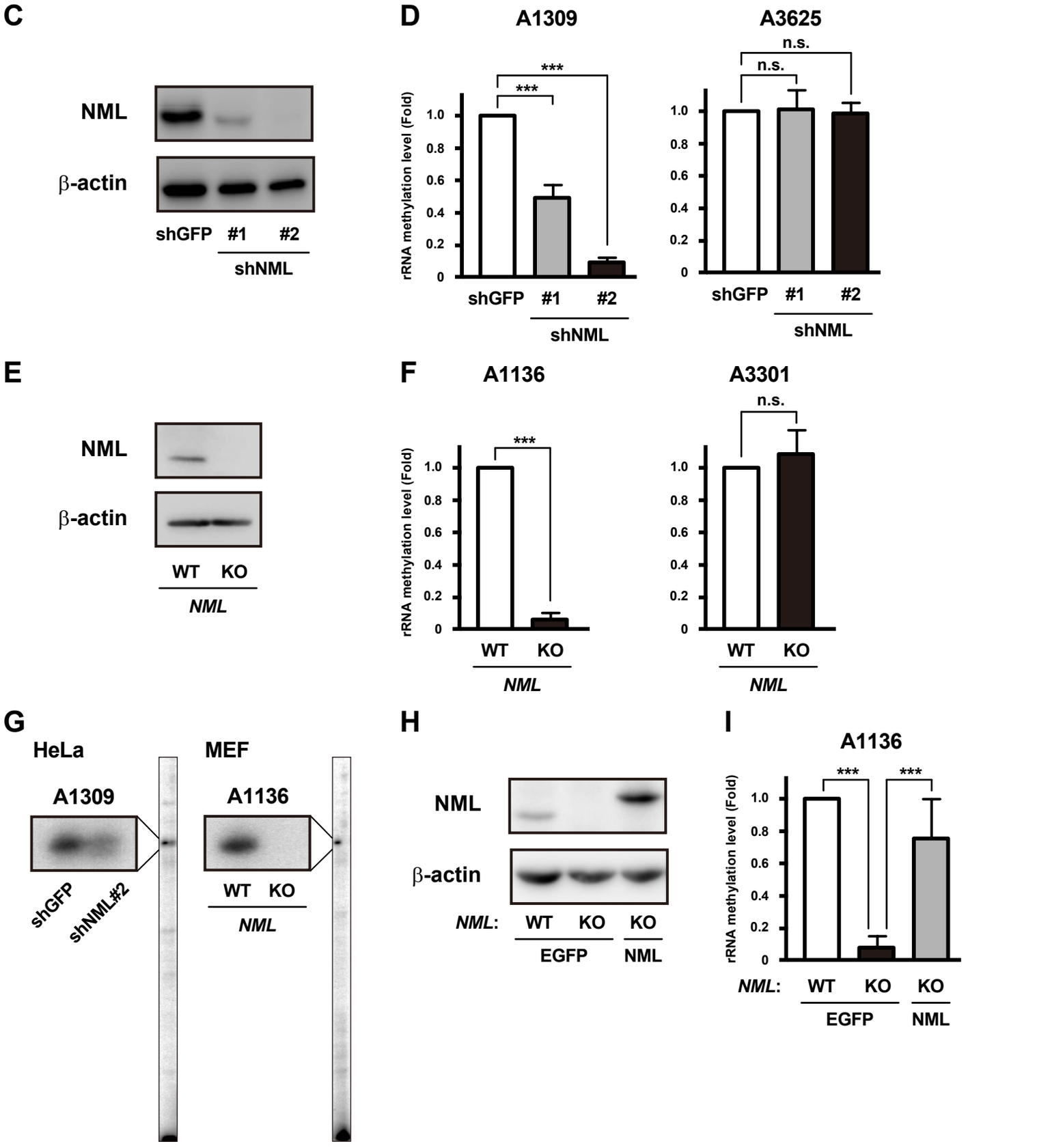


**(C, D)** Methylation levels around a region of 28S rRNA, including A1309 or A3625, in HeLa cells expressing shRNAs targeting *GFP* (shGFP) or *NML* (shNML#1 or #2) were analyzed by qRT-PCR analysis (D). shGFP was used as a control shRNA. Protein levels of NML in the indicated cells were determined by Western blotting (C). Mean values ± S.D. are shown (n = 3). ***$P$ < 0.005; n.s., not significant (bootstrap and permutation tests).

**(E, F)** Methylation levels were measured by qRT-PCR analysis around a region of 28S rRNA, including A1136 or A3301, in *NML* WT or KO immortalized MEFs (F). NML protein levels were determined by Western blotting (E). Mean values ± S.D. are shown (n = 3). ***$P$ < 0.005; n.s., not significant (bootstrap and permutation tests).

**(G)** Modification states at A1309 of human 28S rRNA in shGFP- or shNML#2-expressing HeLa cells and at A1136 of mouse 28S rRNA in *NML* WT or KO immortalized MEFs, were analyzed by primer extension method.

**(H, I)** Expression of FLAG-HA-tagged NML recoverd the methylation levels around A1136 of 28S rRNA in *NML* KO immortalized MEFs, were demonstrated by Western blotting (H) and qRT-PCR analysis (I). Mean values ± S.D. are shown (n = 3). ***$P$ < 0.005 (bootstrap and permutation tests).

# Fig. II-3

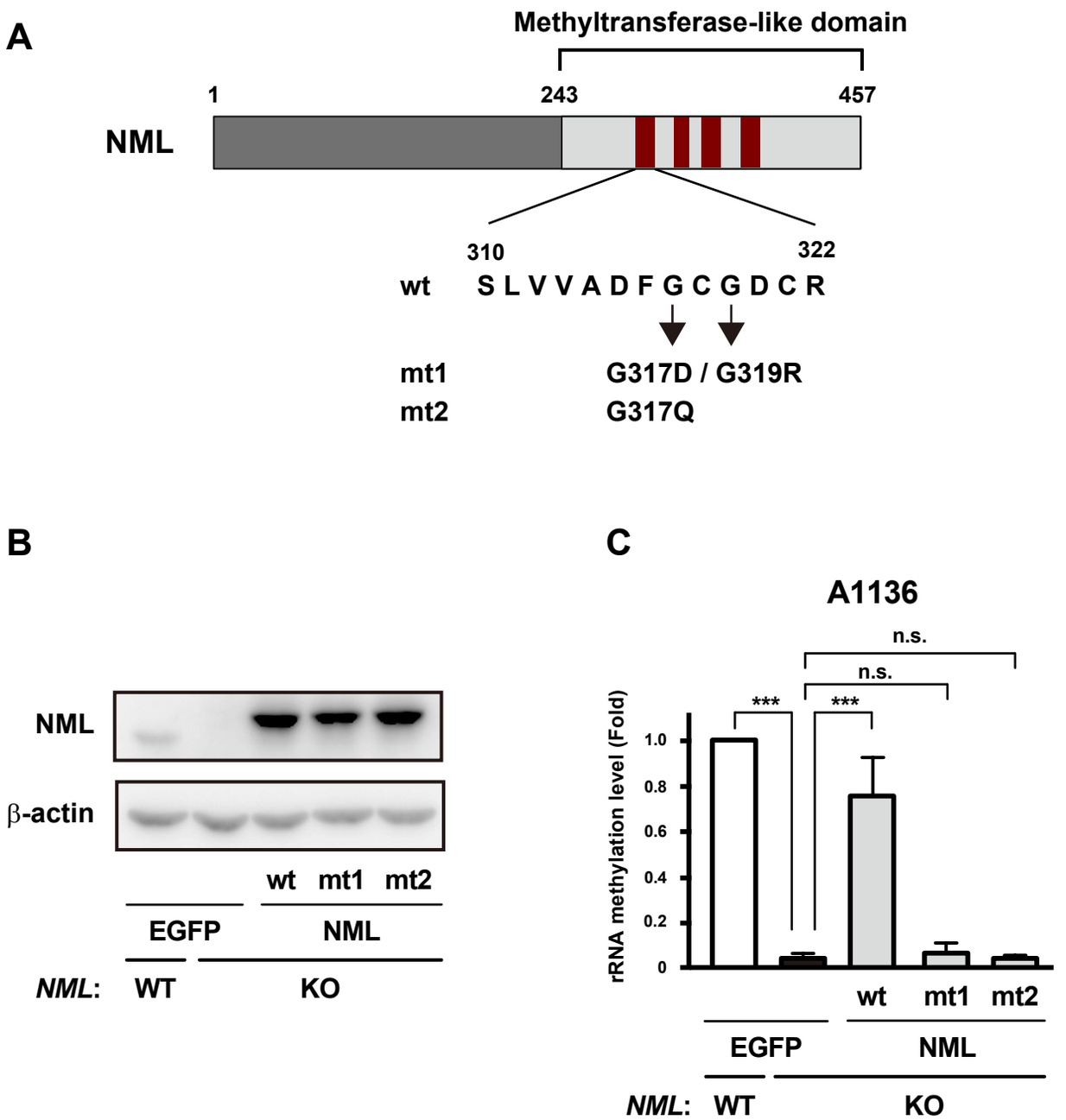


**Fig. II-3 NML regulates rRNA methylation through its Rossmann-fold methyltransferase-like domain.**

**(A)** Schematic representation of wild-type (wt) and point mutant NML are indicated. The mutations were induced in the Rossmann-fold methyltransferase-like domain (mt1 and mt2). Conserved motifs in the SAM dependent-methyltransferase are shown as the red bars.

**(B)** Protein levels of NML in *NML* WT or KO immortalized MEFs expressing EGFP or FLAG-HA-tagged NML were analyzed by Western blotting.

**(C)** Methylation levels around A1136 of 28S rRNA in the indicated cells were measured by qRT-PCR analysis. Mean values ± S.D. are shown (n = 3). ***$P < 0.005$; n.s., not significant (bootstrap and permutation tests).

# Fig. II-4

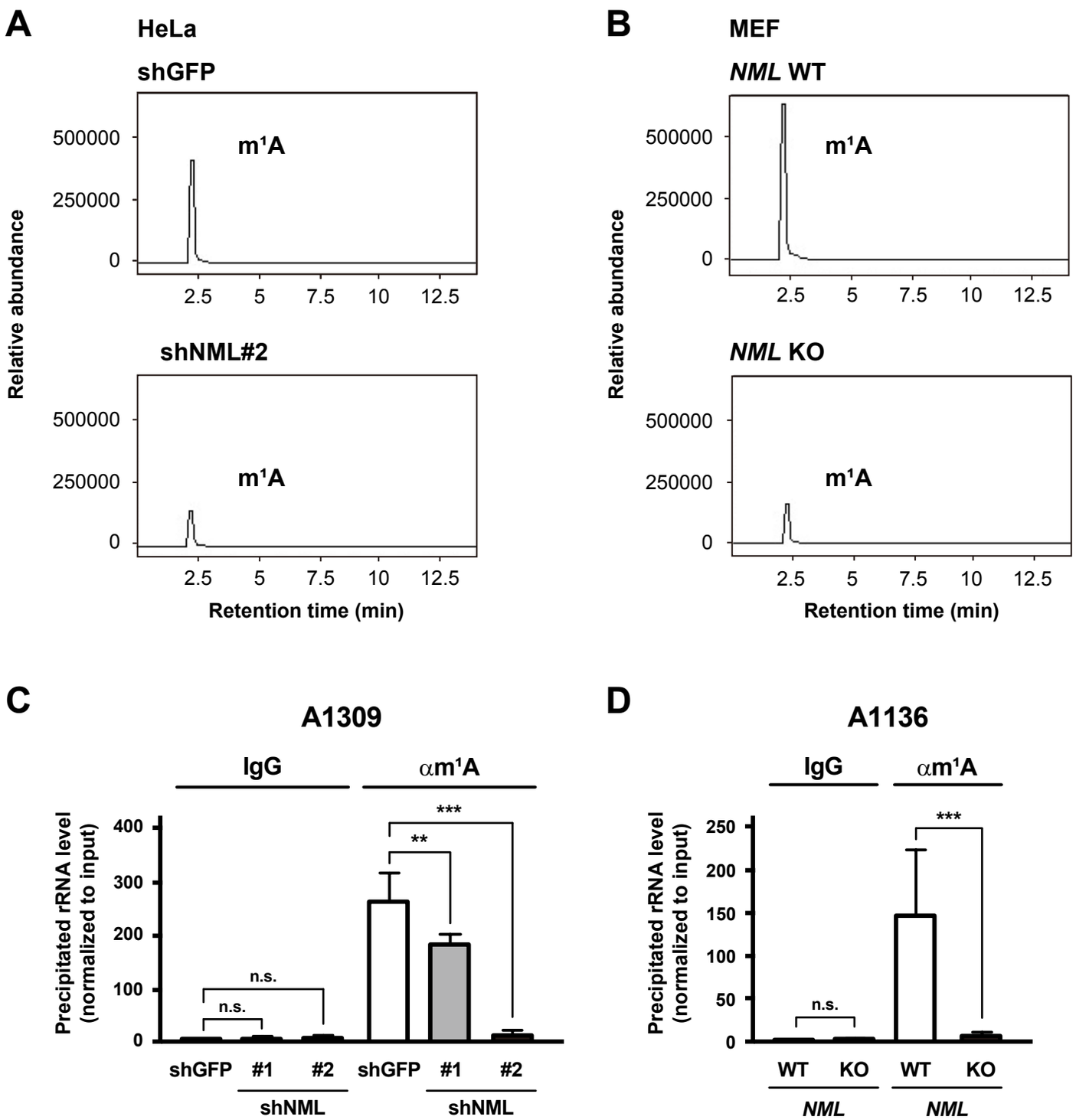


**Fig. II-4 NML is related to m¹A modification in 28S rRNA.**

**(A, B)** The amount of m¹A modified ribonucleosides in 28S rRNA of shGFP or shNML#2 transfected HeLa cells (A) and of *NML* WT or KO immortalized MEFs (B) was analyzed by LC-MS/MS.

**(C, D)** The m¹A levels around A1309 in 28S rRNA of shGFP-or shNML#2-expressing HeLa cells (C) and around A1136 in 28S rRNA of *NML* WT or KO immortalized MEFs were investigated by RIP using an anti-m¹A antibody (αm¹A). An unconjugated affinity purified IgG from mouse was used as a control. Mean values ± S.D. are shown (n = 3). $^{**}P < 0.01$; $^{***}P < 0.005$; n.s., not significant (one-way ANOVA followed by Tukey's test) in C. $^{***}P < 0.005$; n.s., not significant (Student's *t*-test) in D.

# Fig. II-5

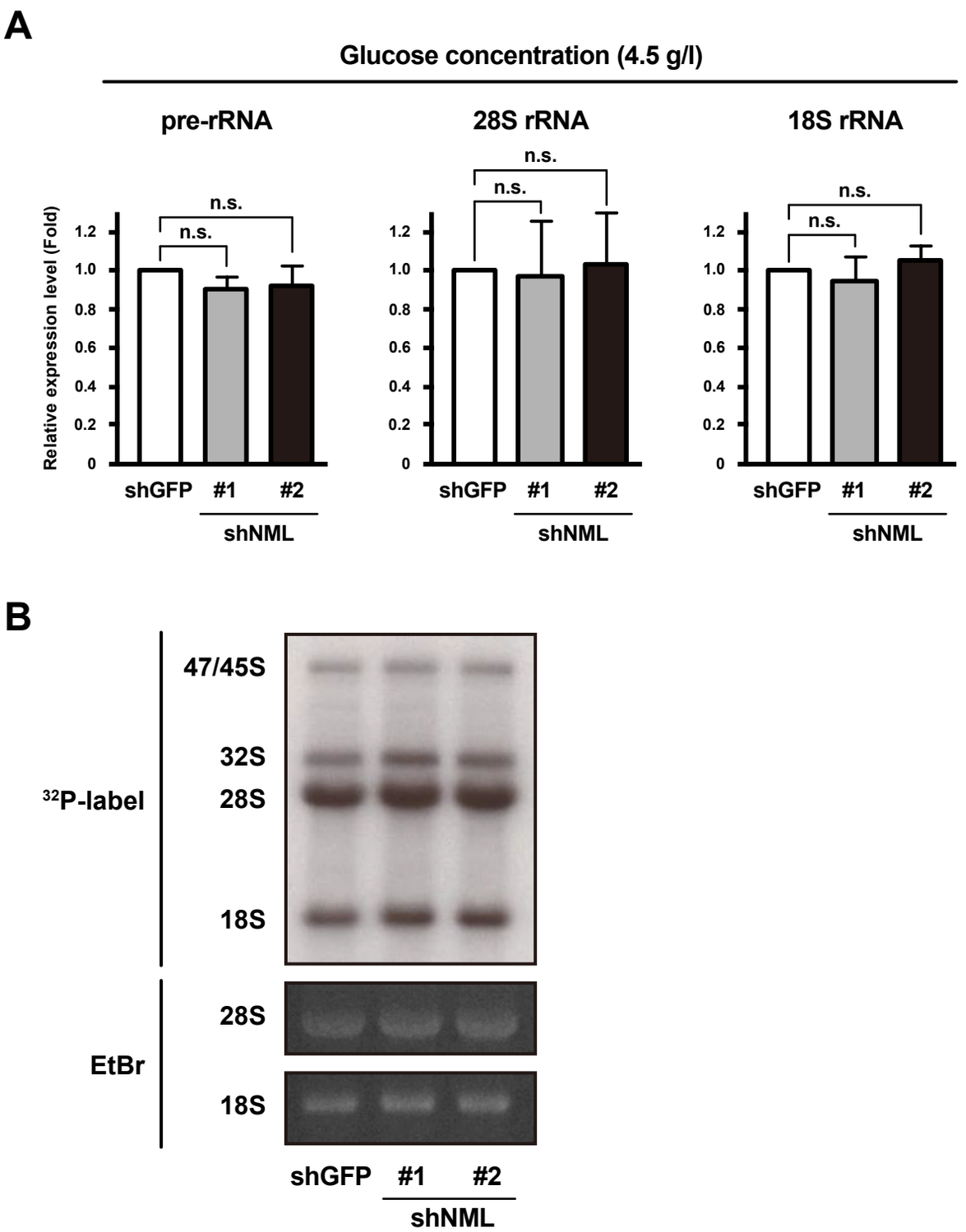


**Fig. II-5 NML does not affect the state of rRNA trascription and processing under glucose-rich conditions.**

**(A)** The levels of pre (45S)-, 28S and 18S rRNA of HeLa cells transfected shGFP, shNML#1 or #2 were analyzed by qRT-PCR. Mean values ± S.D. are shown (n = 3). n.s., not significant (bootstrap and permutation tests).

**(B)** The states of RNA processing in the indicated cells were investigated by labeling nascent RNA with $^{32}P$ orthophosphate. The representative images of 28S and 18S rRNA analyzed by agarose gel electrophoresis are also shown.

# Fig. II-6

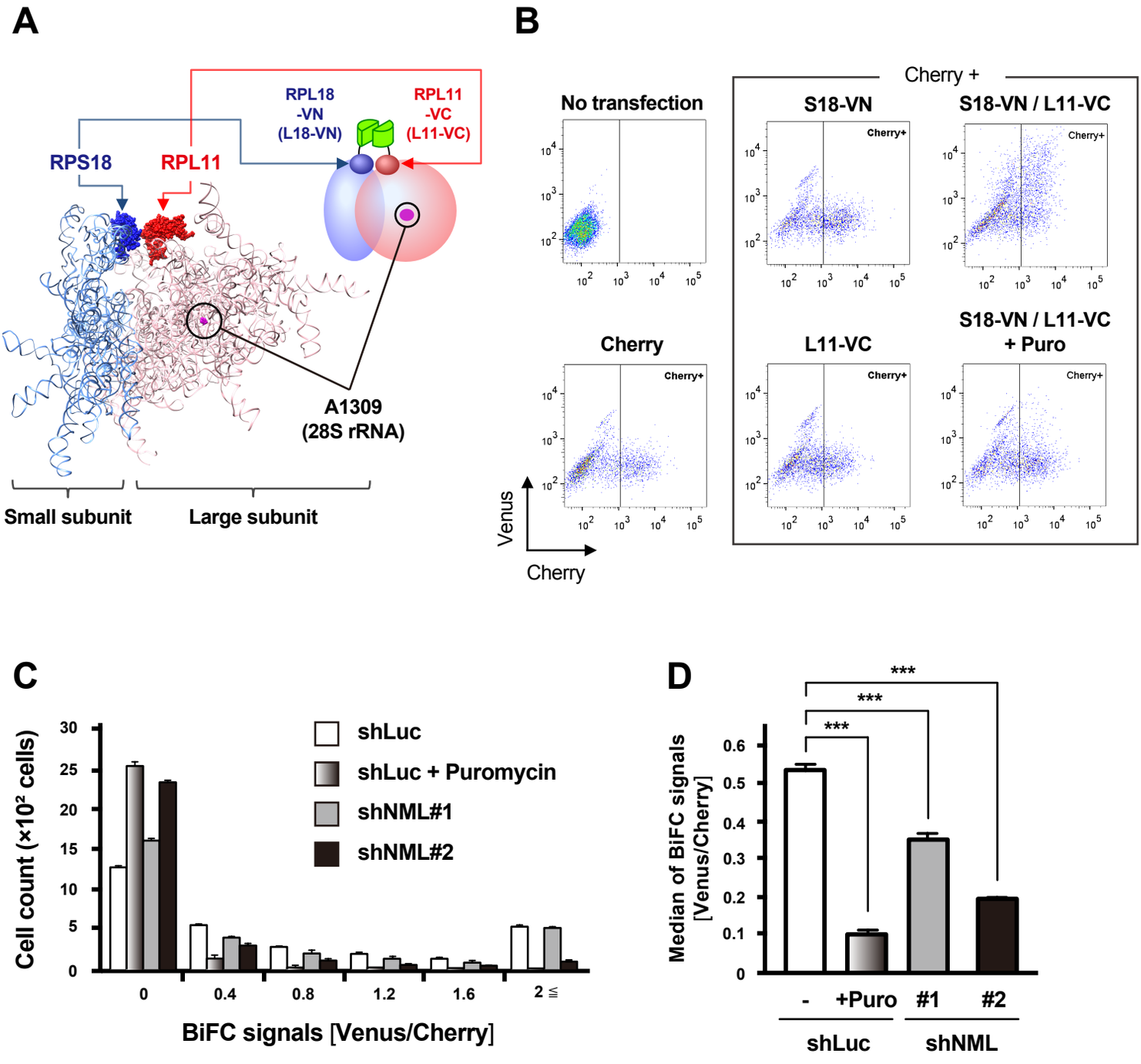


**Fig. II-6 NML reduction suppresses the interaction between ribosomal subunits.**

**(A)** Crystal structure of the human ribosome (Protein Databank ID; 4V6X) are shown. RPS18, RPL11 and A1309 of 28S rRNA are highlighted in different colors. The BiFC model used in this study are also schematically represented. In this model, RPS18 and RPL11 are tagged with the N- or C-terminal parts of Venus, respectively (S18-VN and L11-VC).

**(B-D)** The interaction between ribosomal subunits in HeLa cells transfected shRNA targeting *Luciferase* (shLuc) or *NML* (shNML#1 or #2) was analyzed by BiFC following FACS analysis. The shLuc was used as a control shRNA. S18-VN and/or L11-VC were co-transfected into cells with mCherry as a transfection control marker, and treated with or without puromycin (Puro). Venus and mCherry emissions (BiFC signals) from shLuc-transfected HeLa cells in the indicated conditions detected are indicated in B. The distribution and median of the BiFC signals are shown in C and D, respectively. Mean values ± S.D. are shown (n = 3). ***$P < 0.005$ (one-way ANOVA followed by Tukey's test).

# Fig. II-7

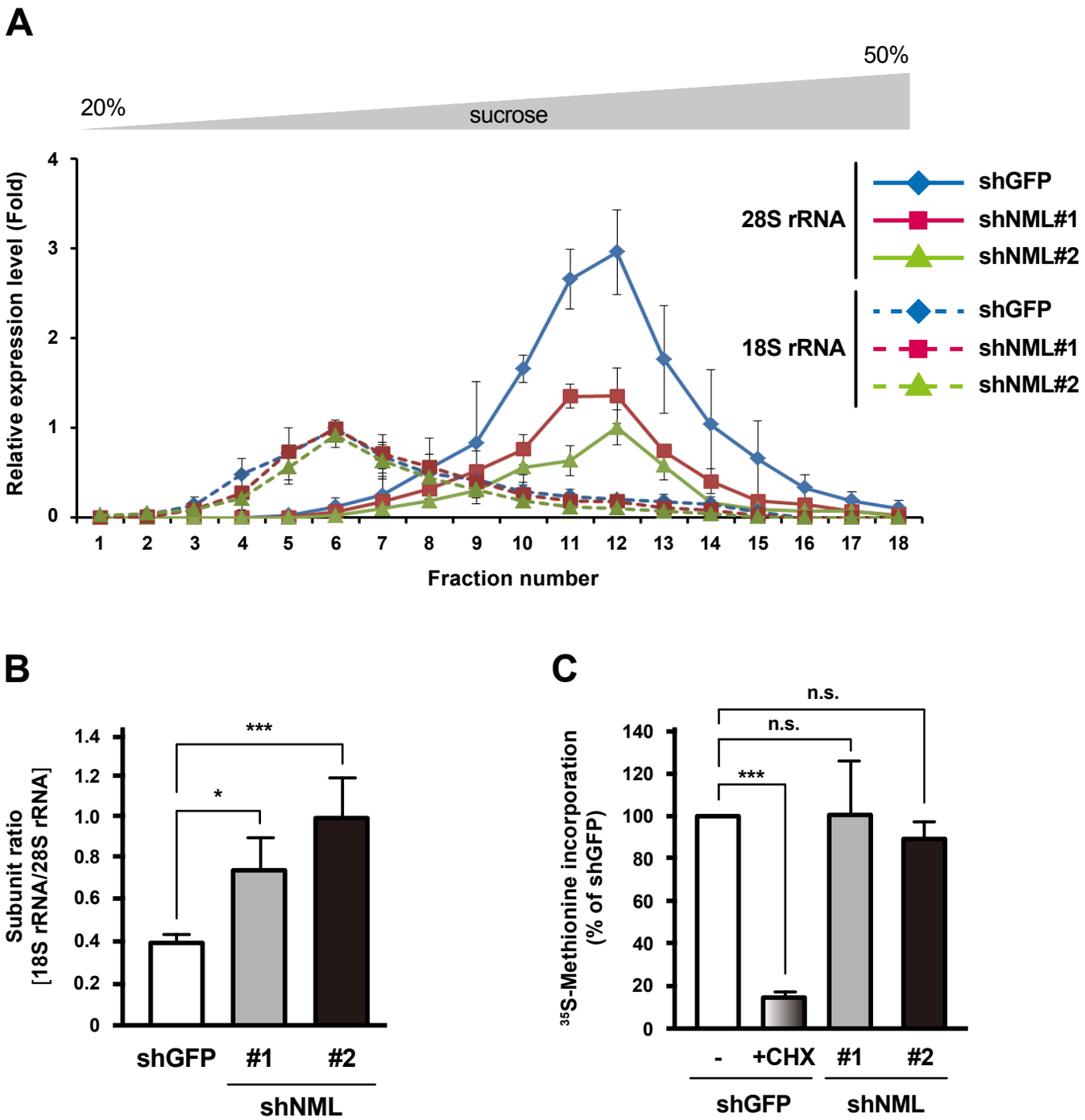


**Fig. II-7 NML participates in the 60S ribosomal subunit formation without affecting the protein synthesis rate.**

**(A, B)** Ribosomal subunit formation in shGFP-, shNML#1- or shNML#2-transfected HeLa cells were analyzed by sucrose density gradient centrifugation following qRT-PCR. 28S and 18S rRNA levels in each fraction were normalized against those obtained with non-centrifugated RNA samples (A). The ratios between the total amounts of 18S and 28S rRNAs are shown as subunit ratios for the indicated cells (B). Mean values ± S.D. are shown (n = 3). **P* < 0.05; ****P* < 0.005; n.s., not significant (one-way ANOVA followed by Tukey's test).

**(C)** The total protein synthesis rates in the indicated cells were measured based on $^{35}$S-Methionine incorporation into newly synthesized polypeptides. Cycloheximide (CHX) was used as a positive control. Mean values ± S.D. are shown (n = 3). ****P* < 0.005; n.s., not significant (bootstrap and permutation tests).

# Fig. II-8

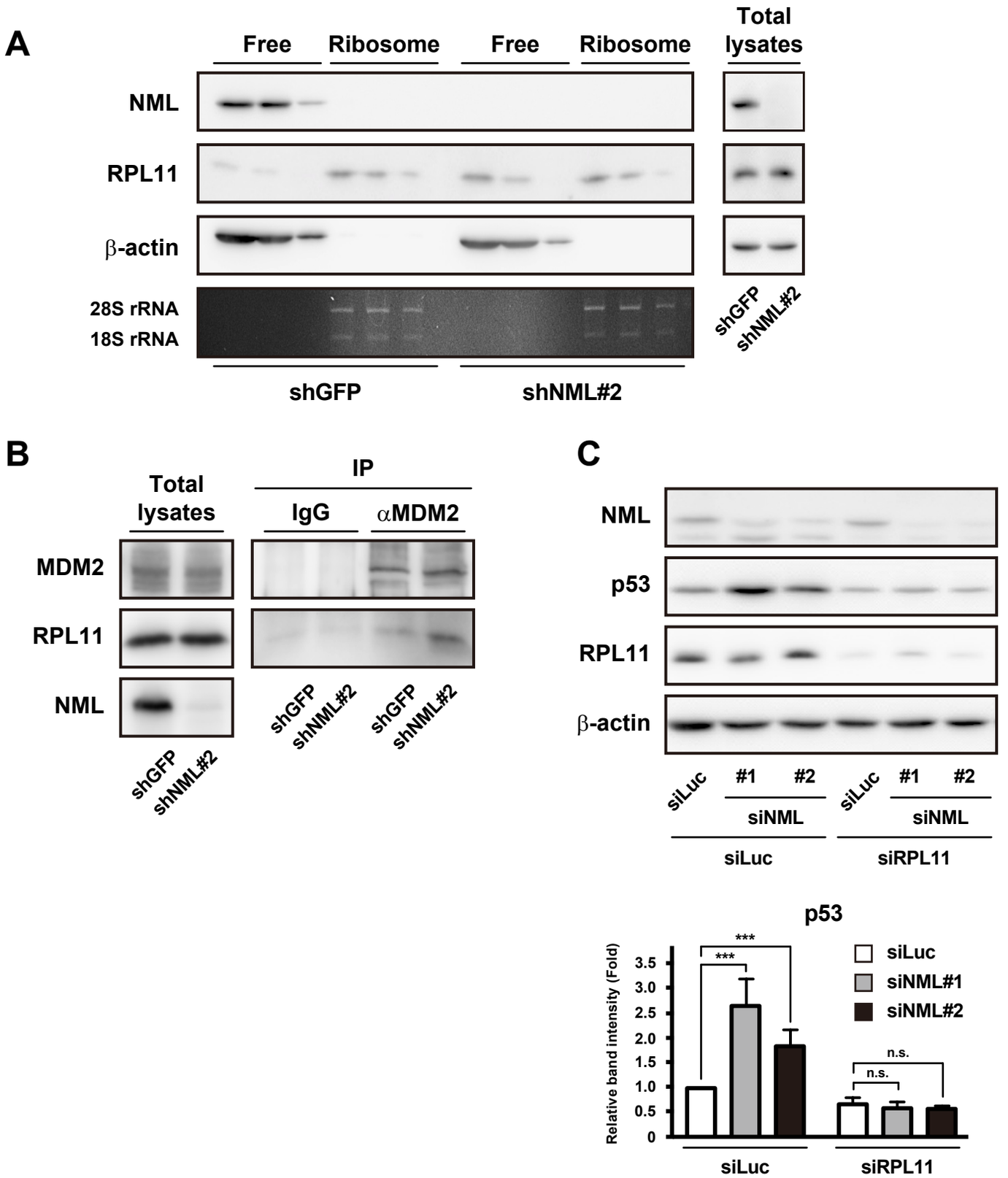


**Fig. II-8 NML depletion increases p53 protein levels through RPL11-mediated mechanism.**

**(A)** Protein levels of RPL11 in the ribosome-free (Free) and ribosomal (Ribosome) fraction of shGFP- or shNML#2-transfected HeLa cells were analyzed by sucrose gradient density centrifugation followed by Western blotting (top three rows). 28S and 18S rRNAs are detected as references for ribosome sedimentation by agarose gel electrophoresis (bottom row).

**(B)** Interaction between RPL11 and MDM2 in shGFP- or shNML#2-transfected HeLa cells was investigated by immunoprecipitation (IP) with an anti-MDM2 antibody (αMDM2) followed by Western blotting. An unconjugated affinity purified IgG from mouse was used as a control for IP.

**(C)** Protein levels of p53 in HCT116 *p53*$^{+/+}$ cells, which were treated with siRNA targeting *Luciferase* (siLuc) or *NML* (siNML#1 or #2) and/or *RPL11* (siRPL11) for two days, were analyzed by Western blotting. Representative Western blotting data are shown. The lower graph indicates the band intensity of p53 normalized that of β-actin. Mean values ± S.D. are shown (n = 3). ***$P$ < 0.005; n.s., not significant (bootstrap and permutation tests).

# Fig. II-9

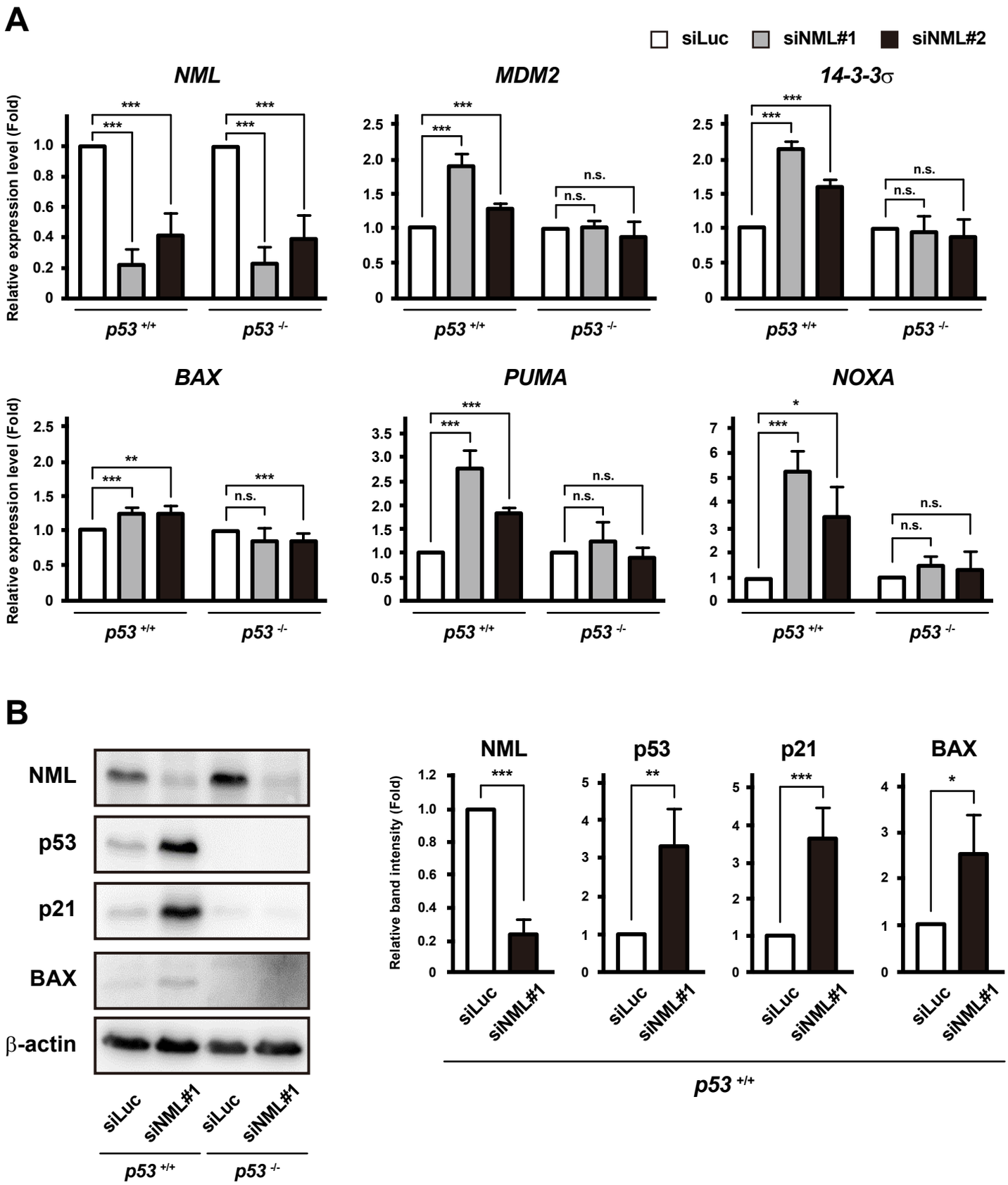


(*Figures and Figure legends continued on next page*)

# Fig. II-9 (*continued*)

## C

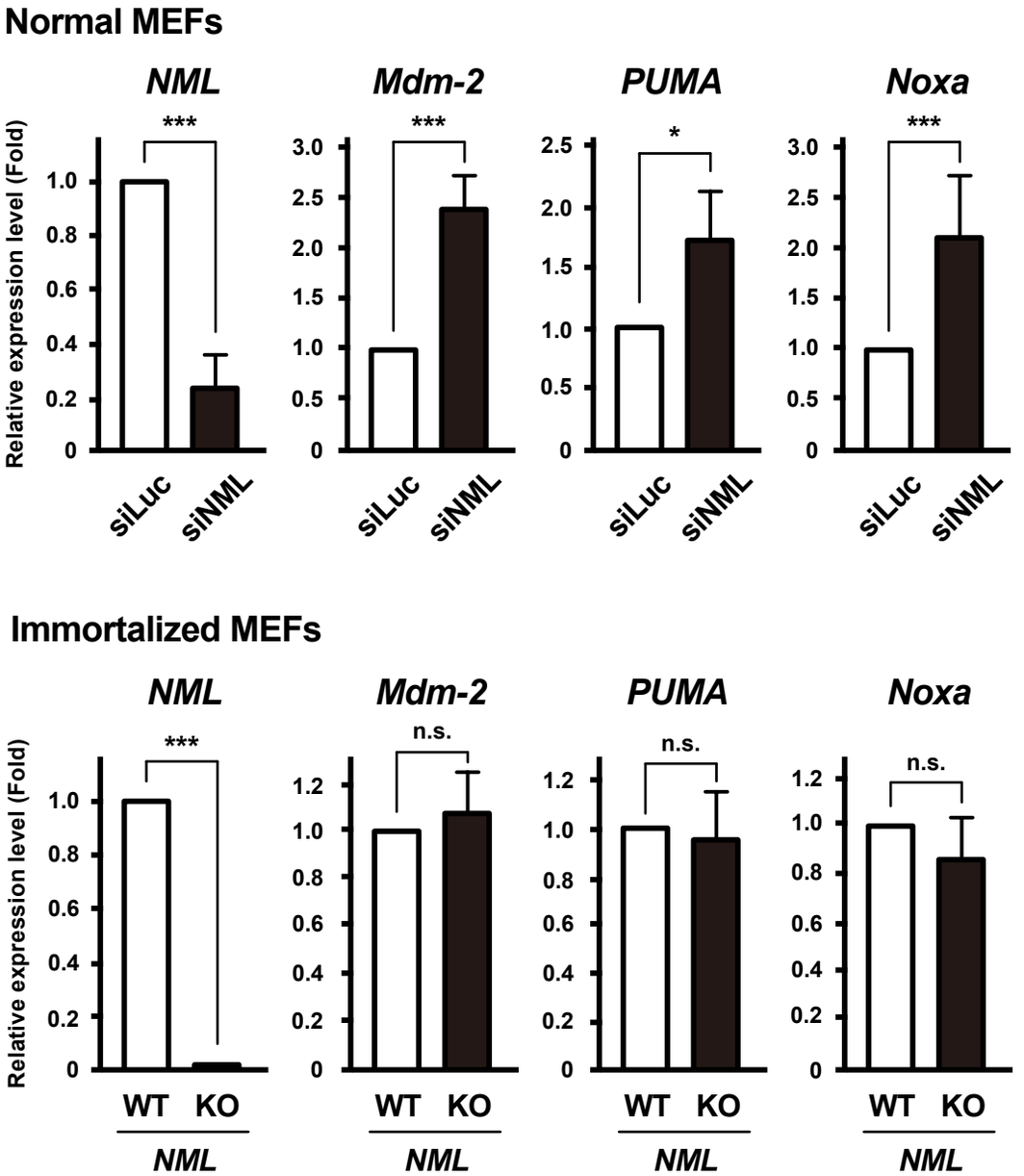


**Fig. II-9 NML depletion induces the activation of p53 pathway.**

**(A)** The mRNA levels of p53 target genes in HCT116 *p53*$^{+/+}$ or *p53*$^{-/-}$ cells, which were treated with siLuc, siNML#1 or siNML#2 for three days, were measured by qRT-PCR. Graphs are indicated as the fold change relative to corresponding mRNA levels in siLuc-transfected HCT116 *p53*$^{+/+}$ or *p53*$^{-/-}$ cells. Mean values ± S.D. are shown (n = 3). **P* < 0.05; ***P* < 0.01; ****P* < 0.005; n.s., not significant (bootstrap and permutation tests).

**(B)** Protein levels of p53 targets in HCT116 *p53*$^{+/+}$ or *p53*$^{-/-}$ cells, which were treated with siLuc or siNML#1 for three days, were analyzed by Western blotting. Representative Western blotting data are shown in the left panel. The right graphs indicate the band intensity of the indicated proteins normalized that of β-actin. Mean values ± S.D. are shown (n = 3). **P* < 0.05; ***P* < 0.01; ****P* < 0.005 (bootstrap and permutation tests).

**(C)** The mRNA levels of p53 target genes in normal and immortalized MEFs (*NML* WT or KO) were investigated by qRT-PCR. In the case of normal MEFs, the cells were treated with siLuc or siNML#1. Three days after transfection, the indicated mRNA levels were analyzed. Mean values ± S.D. are shown (n = 3). **P* < 0.05; ****P* < 0.005; n.s., not significant (bootstrap and permutation tests).

# Fig. II-10

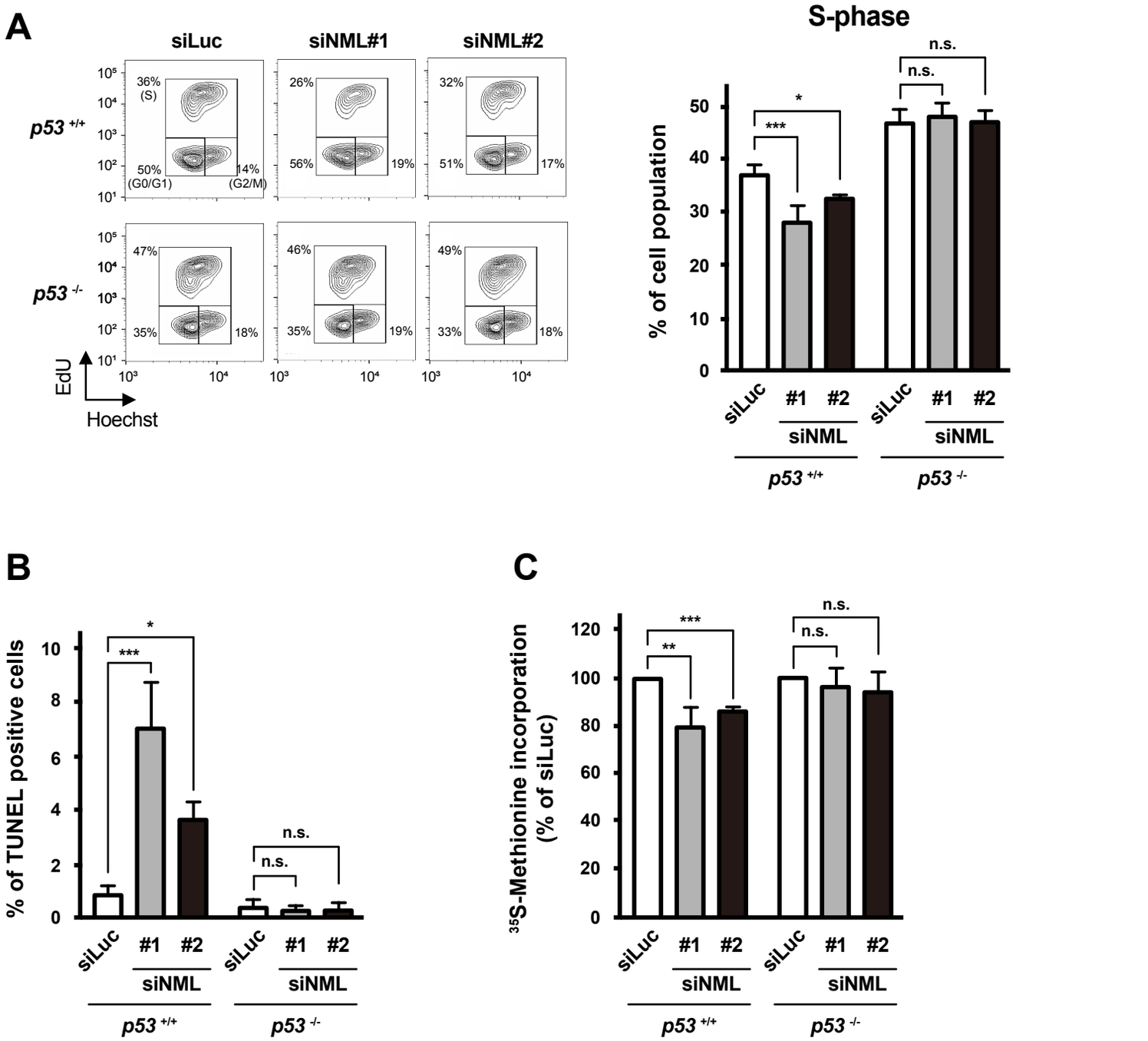


**Fig. II-10 NML reduction induces the p53-dependent cellular events.**

**(A)** Cell cycle analysis of HCT116 *p53*$^{+/+}$ or *p53*$^{-/-}$ cells, which were treated with siLuc, siNML#1 or siNML#2 for three days, were performed by EdU staining following FACS analysis (left panels). The percentages of cell population in the S-phase were compared between the indicated cells, and shown as the graph (right panel). Mean values ± S.D. are shown (n = 3). **P* < 0.05; ****P* < 0.005; n.s., not significant (one-way ANOVA followed byTukey's test).

**(B)** Apoptosis assay of HCT116 *p53*$^{+/+}$ or *p53*$^{-/-}$ cells, which were treated with siLuc, siNML#1 or siNML#2 for three days, were conducted by TUNEL staining. For each group, cells were counted in three randomly selected fields (more than 100 cells/field) per experiment. Mean values ± S.D. are shown (n = 3). **P* < 0.05; ****P* < 0.005; n.s., not significant (one-way ANOVA followed by Tukey's test).

**(C)** The total protein synthesis rates in HCT116 *p53*$^{+/+}$ or *p53*$^{-/-}$ cells, which were treated with siLuc, siNML#1 or siNML#2 for three days, were measured based on $^{35}$S-Methionine incorporation into newly synthesized polypeptides. Mean values ± S.D. are shown (n = 3). ***P* < 0.01; ****P* < 0.005; n.s., not significant (bootstrap and permutation tests).

# Fig. II-11

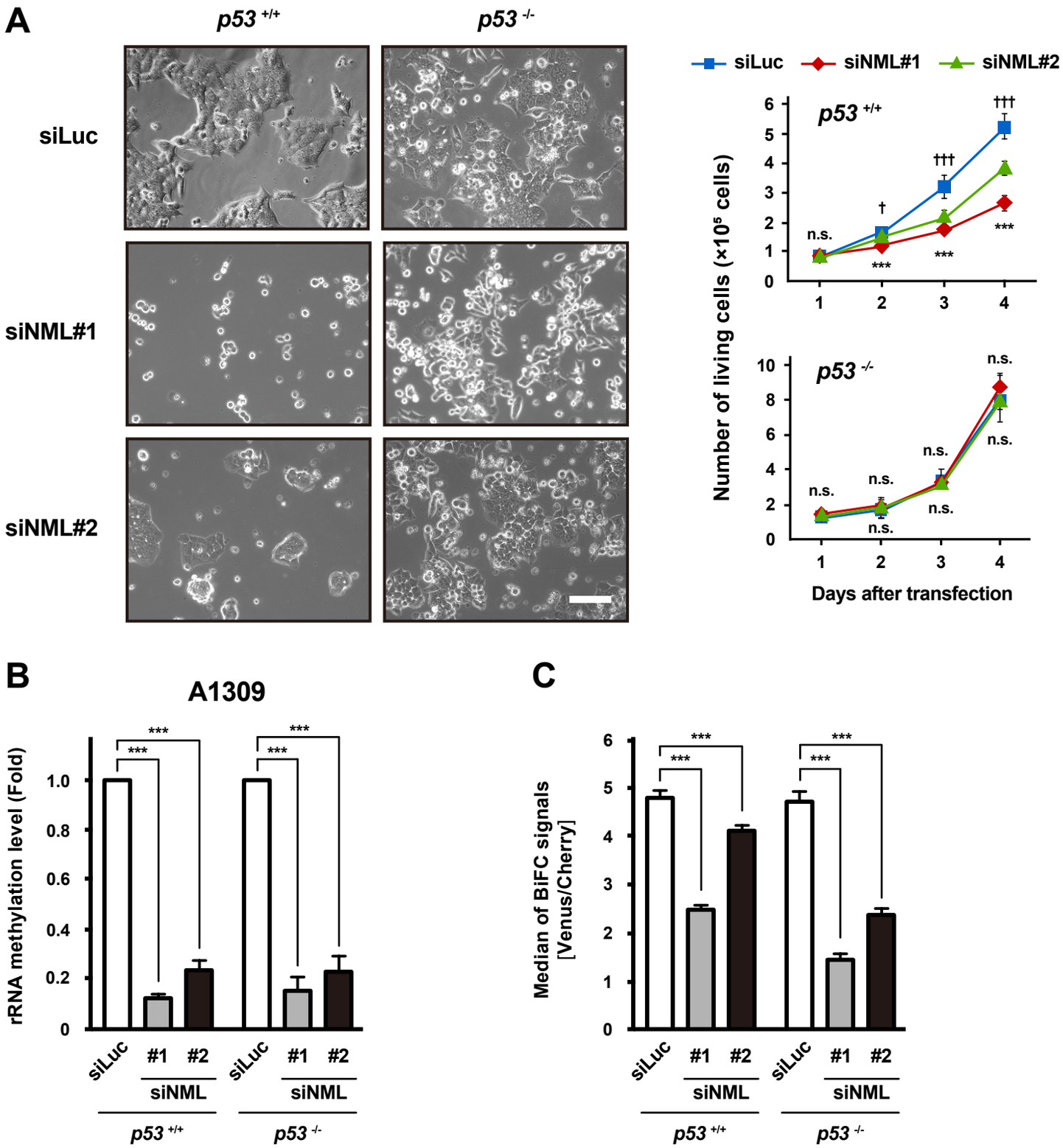


**Fig. II-11 NML regulates cell proliferation in a p53-dependent manner.**

**(A)** Phase-contrast images and growth curves of HCT116 *p53*$^{+/+}$ or *p53*$^{-/-}$ cells, which were treated with siLuc, siNML#1 or siNML#2, are shown. The phase-contrast images (left panels) were taken three days after siRNA transfection. White scale bar: 100 μm. Living cells were automatically counted at the indicated days after transfection by Trypan Blue staining (right panels). The statistical significance between siLuc- and siNML#1- or siNML#2-treated cells is shown by * and †, respectively. Mean values ± S.D. are shown (n = 3). $^{\dagger}P < 0.05$; *** or $^{\dagger\dagger\dagger}P < 0.005$; n.s., not significant (one-way ANOVA followed by Tukey's test).

**(B)** Methylation levels around A1309 of 28S rRNA in HCT116 *p53*$^{+/+}$ or *p53*$^{-/-}$ cells, which were treated with siLuc, siNML#1 or siNML#2 for three days, were measured by qRT-PCR analysis. Mean values ± S.D. are shown (n = 3). ***$P < 0.005$ (bootstrap and permutation tests).

**(C)** The meadian BiFC signals in HCT116 *p53*$^{+/+}$ or *p53*$^{-/-}$ cells, which were treated with siLuc, siNML#1 or siNML#2 for three days, are shown. The BiFC signals were quantified by FACS analysis. Mean values ± S.D. are shown (n = 3). ***$P < 0.005$ (bootstrap and permutation tests).

**Table 1. Primers for qRT-PCR**

| Species | Primer name | Sequence (5' - 3') |
|---|---|---|
| Human | 45S (pre-) rRNA_Fw | CAGGTGTTTCCTCGTACCG |
| | 45S (pre-) rRNA_Rv | CACCCGACCCGTCTTGAAAC |
| | 28S rRNA_Fw | TCATCAGACCCCAGAAAAGG |
| | 28S rRNA_Rv | GATTCGGCAGGTGAGTTGTT |
| | 18S rRNA_Fw | AAACGGCTACCACATCCAAG |
| | 18S rRNA_Rv | CCTCCAATGGATCCTCGTTA |
| | 5S rRNA_Fw | GATCTCGGAAGCTAAGCAGG |
| | 5S rRNA_Rv | AAGCCTACAGCACCCGGTAT |
| | NML_Fw | CCTAGAGGAGGCAAATAGAG |
| | NML_Rv | CAGGTCCTTGGAGACAATC |
| | MDM2_Fw | CATGCCTGCCCACTTTAGA |
| | MDM2_Rv | GGAGGCTCCCAACTGCTT |
| | 14-3-3σ_Fw | TTGTGGCTGAGAACTGGACA |
| | 14-3-3σ_Rv | ACACCCAGCAGACATGCTTT |
| | BAX_Fw | ATGTTTTCTGACGGCAACTTC |
| | BAX_Rv | ATCAGTTCCGGCACCTTG |
| | PUMA_Fw | TTGTGCTGGTGCCCGTTCCA |
| | PUMA_Rv | AGGCTAGTGGTCACGTTTGGCT |
| | NOXA_Fw | GTGCCCTTGGAAACGGAAGA |
| | NOXA_Rv | CCAGCCGCCCAGTCTAATCA |
| | β-actin_Fw | CCAACCGCGAGAAGAT |
| | β-actin_Rv | CCAGAGGCGTACAGGG |

| Species | Primer name | Sequence (5’ - 3’) |
|---|---|---|
| Mouse | NML_Fw | AGTGGACCGTATTGCCAAAGATC |
| | NML_Rv | ATCAAAACAGTGCACAGGGTTCC |
| | Mdm-2_Fw | CTCTGGACTCGGAAGATTACAGCC |
| | Mdm-2_Rv | CCTGTCTGATAGACTGTCACCCG |
| | PUMA_Fw | GTACGAGCGGCGGAGACAAG |
| | PUMA_Rv | GCACCTAGTTGGGCTCCATTTCTG |
| | Noxa_Fw | GAAGTCGCAAAAGAGCAGGATGAG |
| | Noxa_Rv | TGCCGTAAATTCACTTTGTCTCCA |
| | Cyclophilin_Fw | TGCCAGGGTGGTGACTTTACA |
| | Cyclophilin_Rv | GCCATCCAGCCATTCAGTCTTG |

**Table 2. Primers for the site-specific semi-quantitative RT-PCR**

| Species | Primer name | Sequence (5' - 3') |
|---|---|---|
| Human | A1309_RT | CGGCCTTCACCTTCATTG |
| | A1309_Fw | CACCCGACCCGTCTTGAAAC |
| | A1309_Rv | ACTCGCGCACGTGTTAGAC |
| | A3625_RT | CGCGCTTCATTGAATTTCTT |
| | A3625_Fw | CAGGGGAATCCGACTGTTTA |
| | A3625_Rv | CGCGCTTCATTGAATTTCTT |
| Mouse | A1136_RT | GGCCCTTCACCTTCATTG |
| | A1136_Fw | CACCCGACCCGTCTTGAAAC |
| | A1136_Rv | CCTGACTCGCGCACGCGTTA |
| | A3301_RT | CGCGCTTCATTGAATTTCTT |
| | A3301_Fw | CAGGGGAATCCGACTGTTTA |
| | A3301_Rv | CGCGCTTCATTGAATTTCTT |

## Chapter III.

# Identification of rRNA adenine methyltransferase-1 (RRAM-1) as $m^1A$ modification factor in *Caenorhabditis elegans*

## Abstract

RNAs are post-transcriptionally modified in all kingdoms of life. The RNA modifications play important roles in the regulation of RNA stability and function. Of these modifications, base methylations are highly conserved in eukaryote ribosomal RNA (rRNA). Recently, yeast rRNA processing protein 8 (Rrp8) and mammalian nucleomethylin (NML) were identified as factors of $N^1$-methyladenosine ($m^1A$) modification in yeast 25S and mammalian 28S rRNA, respectively. However, the physiological role of $m^1A$ modification in rRNA is still poorly understood.

Here, using the liquid chromatography/tandem mass spectrometry (LC-MS/MS) analysis and RNA immunoprecipitation (RIP) assay, I identified that an $m^1A$ modification is located around position 674 (A674) of *Caenorhabditis elegans* (*C. elegans*) 26S rRNA. Furthermore, quantitative PCR-based analysis revealed that T07A9.8, a *C. elegans* homolog of yeast Rrp8 and mammalian NML, is responsible for the $m^1A$ modification at A674 of 26S rRNA. This $m^1A$ modification site in *C. elegans* corresponds with those in yeast 25S rRNA and mammal 28S rRNA. Intriguingly, T07A9.8 is not associated with transcription and processing of rRNA under normal

nutrient conditions. Because of the functional diversities among T07A9.8, Rrp8, and NML, I renamed the *T07A9.8* gene as *rRNA adenine methyltransferase-1* (*rram-1*).

The further *in vivo* analysis demonstrated that RRAM-1 reduction induces autophagy and significantly extends the lifespan under normal feeding environments.

Thus, my findings suggest that the $m^1A$ modification of 26S rRNA contributes to the regulation of autophagy and lifespan in *C. elegans*.

## Introduction

RNA functions as a fundamental molecule that conveys the genetic information from DNA into protein. In each steps, messenger RNA (mRNA) is transcribed from DNA and translated by ribosome that is composed of ribosomal RNAs (rRNAs) and ribosomal proteins. During translation, transfer RNAs (tRNAs) bring specific amino acids to elongating polypeptides through codon-specific pairing with mRNA on the ribosomes. Therefore, RNAs represent central factors throughout the gene expression processes.

RNAs are modified post-transcriptionally in all kingdoms of life. To date, more than 100 different types of modifications have been identified (1, 18, 78). These modifications play roles in structural and functional control of RNA, cellular homeostasis maintenance, stress response, development, and so on (16, 58, 59, 79-81). Furthermore, the fields of RNA modification have been noted owing to the discoveries that some RNA modifications are dynamically and reversibly regulated (82-85). Although a wide variety of RNA modifications exist, 'RNA methylation' accounts for approximately two third of the known chemical modifications occurring with RNAs. The methylations of RNA are induced at almost all nitrogen of the nucleobases (base methylation) and also at the oxygen of the ribose 2'-OH (2'-*O*-ribose methylation) (86). Since the methods for detection and quantification of RNA methylation is highly

developed, new enzymes and modification sites are rapidly identified (87).

Among these modifications, $N^1$-methyladenosine ($m^1A$) modification was first discovered in yeast total RNA (88) and later found in tRNAs and rRNAs from several species (4, 89). These modifications have been shown to modulate the structural stability and function of these RNAs (3, 90). Within a few years, it has been reported that $m^1A$ modifications present in mRNAs and also they are reversibly regulated by the methyltransferases and demethylases (91-94). Thus, these findings further emphasize the biological significance of this modification. However, the physiological functions of $m^1A$ modification are poorly understood.

Nucleomethylin (NML) is a nucleolar protein that modulates rRNA transcription through the epigenetic regulation and protects cells from energy deprivation-induced apoptosis (39). In addition to this function, as described in chapter II, I have revealed that NML regulates the $m^1A$ modification of 28S rRNA, thereby modulating the ribosomal subunit formation and cell proliferation in mammalian cells (95). Although the cellular functions of NML were investigated, its contribution to *in vivo* events as an $m^1A$ modification factor is largely unknown.

*Caenorhabditis elegans* (*C. elegans*) is a small nematode. Because of its short life cycle (about 2-3 weeks), *C. elegans* is a suitable model organism for fundamental

biological studies, such as development, behavior and aging (7, 8). Furthermore, the genetic and metabolic pathways between *C. elegans* and mammals are highly conserved (96, 97). Indeed, database searching for *C. elegans* proteins has revealed that T07A9.8 is a putative homolog of yeast Rrp8 and mammalian NML, which are responsible for the $m^1A$ modification of yeast 25S and mammalian 28S rRNA, respectively (57). However, the presence of $m^1A$ modification in *C. elegans* 26S rRNA and the contribution of T07A9.8 to this modification remain to be elucidated.

Here, using a RIP assay and a site-specific semi-quantitative RT-PCR analysis, I showed that T07A9.8 is required for the $m^1A$ modification of 26S rRNA without changing the rRNA transcription. On the basis of its function, I renamed the *T07A9.8* gene as *rRNA adenine methyltransferase-1* (*rram-1*). As a physiological function of *rram-1*, I observed that RRAM-1 is involved in lifespan regulation. Moreover, RRAM-1 reduction induced the autophagosome formation, which might link rRNA $m^1A$ modification to the regulation of lifespan.

## Materials and Methods

### Worms

Worm strains were maintained as described previously (98, 99). The Bristol N2 strain was obtained from the *Caenorhabditis* Genetics Center and used as a wild-type strain in this study. The bacterial strain *E. coli* OP50 was used as a food source for *C. elegans*.

### RNA interference experiment

*T07A9.8* #1 RNAi clone was isolated from Ahringer's RNAi library and verified by sequencing the insert. For *T07A9.8* #2 clone, a 500-bp nucleotide fragment, nucleotides 21-520 of the *T07A9.8* gene, was amplified. The *T07A9.8* DNA fragment was cloned into the RNAi feeding vector L4440. The primer sequences for amplification of the fragment were as follows:

Forward primer, 5'- TACGGATGAAAAGGATGCTC -3'

Reverse primer, 5'- CAGCAAATCCCTTGTGATAT -3'.

HT115 (DE3) bacteria were transformed with the RNAi vector expressing dsRNA of the genes of interest and cultured on LB plates with 50 μg/ml ampicillin and 10 μg/ml tetracycline. Each single colony was inoculated in 3 ml of LB containing ampicillin and grown for 6-12 h. These cultures were seeded on NGM plates containing

25 μg/ml carbenicillin and 1 mM isopropylthiogalactoside. To induce dsRNA expression, these plates were incubated at room temperature overnight. Worms grown on these RNAi plates were harvested and used for experiments.

## Antibodies

The following antibodies were used in my study: anti-β-actin (M177-3; MBL, Japan); anti-1-methyladenosine (D345-3; MBL); anti-LC3 (PM036; MBL); anti-GFP (D5.1) XP (#2956; Cell Signaling Technology, USA); and normal mouse IgG (sc-2025; Santa Cruz Biotechnology, USA). The rabbit anti-*C. elegans* T07A9.8 antibody was raised against a synthetic peptide corresponding to 30-45 amino acids of the T07A9.8 protein. A rabbit anti-mouse NML antibody was previously prepared (40). Horseradish peroxidase-linked (HPL) sheep anti-mouse IgG (NA931; GE Healthcare, UK) and HPL donkey anti-rabbit IgG (NA934; GE Healthcare) were used as secondary antibodies for Western blotting.

## Quantification of methylated ribonucleosides with liquid chromatography/tandem mass spectrometry (LC-MS/MS)

Large RNAs were extracted with ISOGEN II (Nippon Gene, Japan) according to the manufacturer's protocols. To quantify the methylated ribonucleotides in rRNA, 26S

rRNA and 18S rRNA were isolated from large RNAs by performing agarose gel electrophoresis and gel extraction with the NucleoSpin® Gel and PCR Clean-up system (MACHEREY-NAGEL, Germany) according to the instruction manual. One unit of nuclease P1 (Wako Pure Chemicals, Japan) was added to the heat-denatured RNA sample (1 to 2 μg) in 10 mM ammonium acetate buffer (pH 5.3) and then incubated for 2 h at 45 °C. Subsequently, the sample was dephosphorylated by additions of venom phosphodiesterase I (0.0002 unit, Sigma, USA) and bacterial alkaline phosphatase (0.3 unit, Toyobo, Japan) in 0.1 M ammonium bicarbonate buffer (pH 7.9) for 2 h at 37 °C, as previously described (45). As an internal standard, 10 pmol of 5-bromouridine ($br^5U$, Tokyo Chemical Industry Co., Ltd., Japan) were added into the digestion mixture and enzyme proteins were subsequently removed by acetone precipitation. The supernatant was evaporated to dry up and the resulting nucleoside residues were dissolved with 15 μl of HPLC-grade water (Wako Pure Chemicals).

LC-MS/MS analyses were performed on a Shimadzu Nexera™ UHPLC system coupled to LCMS-8050™ triple quadrupole mass spectrometer (Shimadzu, Japan). LC separations were carried out on a Inertsil ODS-HLTM column (3 μm, 2.1 × 150 mm, GL Science, Japan) with a Inertsil ODS-HLTM Cartridge Guard Column (3 μm, 3.0 × 10 mm, GL Science) at 30 °C, with a flow rate of 0.2 ml/min. The mobile phase

consisted of solvent A (0.1% formic acid) and solvent B (0.1% formic acid in 80% acetonitrile). The water-dissolved samples (5 μl) were injected and eluted starting with 100% solvent A / 0% solvent B for 6 min, followed by a 20 min linear gradient of 0 to 10% solvent B, an one min linear gradient of 10% to 100% solvent B, 5.5 min with 100% solvent B, and 6 min re-equilibration with the initial mobile phase conditions. For determining of elution positions of ribonucleosides on the chromatogram, standard chemicals of adenosine (A, Sigma), $m^1A$ (Santa Cruz Biotechnology), cytidine (C, Sigma), 5-methylcytidine ($m^5C$, Sigma), and $br^5U$ were used, and their retention times were revealed as 19.45 min, 9.47 min, 3.9 min, 9.12 min, and 24.0 min, respectively.

The mass spectrometer was operated using an ion-spray source at 300 °C in the positive mode with unit resolution for Q1 and Q3, and other optimized parameters as follows: interface voltage, 4.0 kV; interface current, 0.1 μA; flow rate of nebulizer gas, 3 l/min; flow rate of heating gas, 10 l/min; flow rate of drying gas, 10 l/min; collision gas (Ar), 270 KPa; DL temperature, 250 °C; heat block temperature, 400 °C; conversion dynode potential, 10 kV; detector potential, 2.44 kV. The multiple reaction monitoring (MRM) transitions and parameters (cone voltage and collision energy of precursor and product ions, respectively) for each nucleoside is listed in Methylated nucleosides database (MNSDB, http://www.agbi.tsukuba.ac.jp/~akiftara/MNSDB/).

## qRT-PCR

Total RNA was extracted using ISOGEN II (Nippon Gene) and treated with DNase I (Nippon Gene) according to the manufacturer's instructions. Extracted total RNA (1 μg) was reverse transcribed with random primers (TaKaRa, Japan) and ReverTra Ace (Toyobo) according to manufacturer's protocols. The qRT-PCR was performed with SYBR *Premix Ex Taq* II (TaKaRa) and the Thermal Cycler Dice Real Time System (TaKaRa). Each gene-expression level was normalized to the *act-1* expression level.

## Western blotting

Worms were lysed in RIPA buffer [20 mM Tris-HCl (pH 7.5), 150 mM NaCl, 2 mM EDTA, 0.8% NP-40, 0.1% SDS, 0.5% sodium deoxycholate] containing protease inhibitor cocktail (Nacalai Tesque, Japan). The extracts were subsequently separated by 10% or 15% SDS-PAGE. The proteins were transferred to Immobilon-P polyvinylidene difluoride transfer membranes (Millipore, USA). After blocking with 0.3% skim milk containing TBS-T buffer [20 mM Tris-HCl (pH 7.5), 150 mM NaCl, 0.1% Tween-20] for 1 h at room temperature, the membranes were incubated overnight at 4 °C with the indicated primary antibodies. After washing with TBS-T buffer, the membranes were

incubated with HRP secondary antibodies for 1 h at room temperature and then washed again with TBS-T buffer. Protein signals were detected with Luminata Forte Western HRP substrate (Millipore).

## RIP experiment

Total RNA extracted from worms were fragmented using the NEBNext Magnesium RNA Fragmentation Module (New England BioLabs, USA). After ethanol precipitation with 20 μg of glycogen, fragmented RNAs were resuspended in IPP buffer [10 mM Tris-HCl (pH 7.5), 150 mM NaCl, 0.1% NP-40]. Solutions containing 1 μg anti-$m^1A$ antibody, 50 μl of 50% slurry protein G Sepharose 4 Fast Flow (GE Healthcare), and 950 μl IPP buffer were added to the pre-cleaned RNA solutions. The mixture was rotated overnight at 4 °C. The beads were washed 3 times with IPP buffer and immunoprecipitated RNAs were purified by phenol/chloroform extraction. After ethanol precipitation, RNAs were analyzed by qRT-PCR. Total RNAs were used as input for normalization of qRT-PCR data.

## Site-specific semi-quantitative RT-PCR

Methylation of 26S rRNA was analyzed by the similar method described in chapter II.

Five hundred nanograms of extracted total RNA were reverse transcribed with 50 units of ReverTra Ace (Toyobo), 1.25 μM of the methylated site unanchored or anchored primer, and either low (0.25 μM) or high (250 μM) concentrations of deoxynucleotide triphosphates (dNTPs). The reactions were performed at 42 °C for 60 min, and then stopped by incubation at 99 °C for 5 min. The following qRT-PCR was performed with SYBR *Premix Ex Taq* II and the Thermal Cycler Dice Real Time System. The methylation levels were calculated as $2^{(CT^{low} - CT^{high})}$, where the CT (threshold cycle) value obtained with the qRT-PCR reaction at the low dNTP concentration was normalized to that obtained at the high dNTP concentration.

## Lifespan analysis

I performed lifespan analysis using the wild-type N2 strain as described previously (98, 99). Briefly, I transferred 30-35 synchronized L1 larvae to each RNAi plate, allowed the worms to develop into adults, and then added 300 μl of 0.5 mg/ml fluorodeoxyuridine solution. Worms were kept at 20 °C and transferred to fresh plates every 4-6 days. Worms feeding on bacteria carrying the empty vector (L4440) were used as control. I monitored the worm populations regularly.

## Statistical analysis

Data are presented as the mean ± standard deviation. The statistical significances were determined by one-way analysis of variance (ANOVA), followed by Dunnett's test. A $P$ value < 0.05 was considered statistically significant. For lifespan analysis data, Kaplan-Meier survival curves were plotted, and log-rank statistics were calculated.

## Results

### $m^1A$ modification is present in *C. elegans* 26S rRNA

To evaluate the presence of $m^1A$ modification and quantify its levels in 26S rRNA, I firstly isolated the 26S- and 18S-rRNA, and performed liquid chromatography/tandem mass spectrometry (LC-MS/MS) analysis to measure the RNA modifications. In 26S rRNA, the chromatogram peak corresponding to that from an $m^1A$ chemical standard was clearly detected. Therefore, I next tried to quantify the $m^1A$ modification levels. Additionally, to ensure the $m^1A$ existence, I also assessed the amount of 2'-*O*-methyladenosine (Am) and 5-methylcytidine ($m^5C$), which are modifications identified in *C. elegans* 26S rRNA (23, 100). The ratios of $m^1A/A$, Am/A, and $m^5C/C$ were 0.588% ± 0.164, 1.379% ± 0.084, and 0.954% ± 0.217, respectively. Accordingly, from LC-MS/MS analyzes, I demonstrated that the $N^1$ position methylated adenosine exists in *C. elegans* 26S rRNA.

### Methyltransferase-like domain is highly conserved in *C. elegans* *T07A9.8*

Recently, NML and Rrp8 were identified as enzymes responsible for the $m^1A$ modification of rRNA in humans (reported in chapter II) and yeast, respectively (6, 95).

However, an enzyme that catalyzes this type of modification in nematodes has not been identified. Hence, I conducted a database search of *C. elegans* proteins, based on amino-acid sequence similarity to the mammalian NML protein, and identified a single putative homolog, *T07A9.8*, consistent with a previous report (57). The *T07A9.8* gene encodes a 343-amino acid protein. Alignment of the T07A9.8 amino acid sequence with homologs revealed that T07A9.8 shares 34% and 29% amino acid identity with the human NML and yeast Rrp8 proteins, respectively. Furthermore, I confirmed that the putative RNA methyltransferase domain, composed of four consensus motifs (motif I, post-I, motif II and III), is highly conserved among these proteins.

## T07A9.8 is not involved in the regulation of rRNA transcription

Human NML functions as not only a rRNA methyltransferase, but also an epigenetic suppressor of rRNA gene transcription (39, 95). Therefore, I examined whether this function as a rRNA transcription repressor is conserved in the T07A9.8 protein. At first, I performed the knockdown of *T07A9.8* with two different RNAi clones and revealed that both clones effectively reduced its expression at the mRNA and protein levels. Next, I evaluated pre-rRNA levels in nematodes by RT-PCR. *T07A9.8* RNAi did not induce obvious changes in the pre-rRNA levels. In addition, the qRT-PCR and agarose

gel electrophoresis experiments showed that the levels of three major rRNA species (26S, 18S and 5.8S rRNA) did not significantly altered in *T07A9.8* RNAi worms. Therefore, these observations suggest that T07A9.8 does not contribute to the regulation of rRNA transcription processes under the normal feeding conditions examined in my study.

## $m^1A$ modification exists within the sequences around A674 of 26S rRNA

The two and one $m^1A$ modification sites in 25S rRNA of *S. cerevisiae* (A645 and A2142) and 28S rRNA of *H. sapiens* (A1309) are well conserved in *C. elegans* 26S rRNA. To investigate the participation of T07A9.8 in the $m^1A$ modification of 26S rRNA, I performed RIP assays with an antibody against $m^1A$ to pull down $m^1A$-modified rRNA. And I found that the region adjacent to adenosine at 674 of 26S rRNA was enriched in $m^1A$-precipitated RNA more than that in control IgG. Furthermore, compared to control RNAi, both *T07A9.8* RNAi clones significantly diminished anti-$m^1A$ antibody ($\alpha m^1A$) precipitated-RNA levels. In chapter II, I confirmed that the A3625 of human 28S rRNA correspond to A2142 of yeast 25S rRNA is not modified (95). The RIP assays using primers flanking A2246 of 26S rRNA revealed that the

region around A2246 does not contain the $m^1A$ residues. Considering that yeast *Bmt2*, a responsible factor for $m^1A2142$ modification of yeast 25S rRNA, is not conserved in *C. elegans*, this result is reasonable. Taken together, these data indicated that the $m^1A$ modification occurs around A674 of 26S rRNA and that T07A9.8 is involved in the methylation.

## T07A9.8 is required for $m^1A$ modification at position 674 of 26S rRNA

To further investigate the $m^1A$ modification of 26S rRNA in detail, I performed a site-specific semi-quantitative reverse transcriptase-PCR (qRT-PCR) analysis. This method is based on the principle that modified residues (including $m^1A$ or 2′-*O*-methylation) induce a pause in the reverse transcriptase reaction at low dNTP concentrations, but not at high dNTP concentrations (Chapter II; Fig. II-2B). Consistent with RIP assays, the methylation levels around A674 were clearly detected (15.16 ± 0.47), and RNAi against *T07A9.8* markedly reduced the methylation levels (8.07 ± 0.79 and 6.68 ±1.53 for RNAi constructs #1 and #2, respectively). Therefore, I concluded that adenosine around position 674 of 26S rRNA is methylated at the $N^1$ position via a T07A9.8-dependent mechanism.

Next, to determine the precise position of the modified residue around A674, I

designed some types of specific reverse primers for the RT reaction and qPCR that were shifted several nucleotides neighboring a target site in 26S rRNA. From these analysis, I confirmed that A674 of 26S rRNA is methylated at $N^1$ position through the T07A9.8-mediated regulation. Based on the function of *T07A9.8*, I renamed this gene as *rRNA adenine methyltransferase-1* (*rram-1*).

## RRAM-1 reduction leads to lifespan extension and autophagosome formation

Finally, I explored the physiological function of RRAM-1. Recently, it has been reported that the depletion of *nsun-5*, which is responsible for the $m^5C$ modification of 26S rRNA, induces longevity under a nutrient-restricted condition (23). Furthermore, the genome-wide RNAi screening experiments suggested that inactivation of *T07A9.8* (*rram-1*) gene extends *C. elegans* lifespan (101, 102). Therefore, I evaluated the relation between *rram-1* and the lifespan regulation, and revealed that *rram-1* RNAi significantly increased the mean lifespan by about 12% compared to control RNAi.

The various cellular processes modulating lifespan have been reported (103, 104). Autophagy is a well-conserved cellular recycling system that also plays a key role in anti-aging (9-12). Intriguingly, I noticed that *NML*-knockout immortalized mouse

embryonic fibroblasts (MEFs) exhibited a higher amount of LC3-II expression, which is a well-used indicator for autophagy, compared with *NML* wild-type MEFs. To examine the roles of RRAM-1 in autophagy, I used the transgenic worms carrying GFP::LGG-1, which is a reliable tool for evaluating autophagy (105, 106). Western blotting analysis demonstrated that the amount of phosphatidylethanolamine (PE)-conjugated LGG-1 (PE-GFP::LGG-1), an indicator of autophagosome formation, increased in *rram-1* RNAi worms. These results imply a possible mechanism that *rram-1* knockdown extends the lifespan through modulating autophagy.

## Discussion

In the present study, I showed that $m^1A$ modification is existing at position 674 of 26S rRNA in *C. elegans*. Additionally, my findings indicate that T07A9.8, a *C. elegans* homolog of yeast Rrp8 and human NML, is responsible for this modification without changing rRNA transcription under the normal feeding conditions. Taking the functional diversity into consideration, I designated the *T07A9.8* gene as *rRNA adenine methyltransferase-1* (*rram-1*). Intriguingly, from the lifespan analysis, I confirmed that RNAi-mediated reduction of RRAM-1 induces longevity. From these findings, I suggest the possibility that RRAM-1 links the $m^1A$ modification of rRNA to lifespan regulation. However, to clearly prove this point, further work is needed using methyltransferase activity-deficient RRAM-1 mutant.

Several studies have used a qRT-PCR-based method to examine the presence of methylated residues within RNA using the flanked PCR primers (34, 35, 95). This method is based on the principle that some kinds of modified residues prevent polymerase chain reaction at low dNTP concentrations. However, these studies did not identify the precise position of the modified residue due to the use of a single primer for the RT step. To resolve this issue, I made use of "Reverse Transcription at Low dNTP concentrations followed by PCR (RTL-P) assay" established by Dong *et al.* (107).

Although they detected the PCR products by agarose gel electrophoresis, I successfully detected them by qRT-PCR. In addition, at the RT reaction, I used primers that were shifted one base at a time around a putative modification residue. Intriguingly, when the 3′-end of the primer covers just on the modified residue, the methylation levels detected were markedly reduced. These data suggest that my improved method can be used to identify the position of methylated residues at single-nucleotide resolution. Therefore, this tool will help map RNA modifications, including $m^1A$ and 2′-*O*-methylation.

Yeast Rrp8 and mammalian NML have been identified as a methyltransferase responsible for the $m^1A$ modification of 25S rRNA (6) and 28S rRNA (95), respectively. In this study, I provide evidence that RRAM-1 is required for the $m^1A$ modification at position 674 of 26S rRNA in *C. elegans*. Indeed, the amino acid sequence alignment of RRAM-1 with Rrp8 and NML shows a high degree of conservation in their C-terminal region, which includes the methyltransferase-like domain. Meanwhile, RRAM-1 hardly contributed to the regulation of rRNA transcription under normal nutrient conditions. Mammalian NML binds to histone H3 dimethylated Lsy9 through its N-terminal region and acts as an epigenetic inhibitor of rRNA transcription under low glucose conditions (39). Although I have not yet examined whether RRAM-1 controls rRNA transcription under the nutrient-depleted conditions, a low sequence similarity of the N-terminal

region between RRAM-1 and NML might lead to the functional difference in regard to the regulation of rRNA transcription.

Intriguingly, RNAi-mediated *rram-1* reduction significantly extends the lifespan. Although this finding agrees with the preceding data observed by genome-wide RNAi screening (101, 102), the mechanisms how RRAM-1 regulates the lifespan are largely unknown. Recently, Schosserer *et al.* showed that the reduction of *nsun-5*, which is a responsible factor of $m^5C$ modification of 26S rRNA, increases the lifespan in *C. elegans* under the nutrient-restricted environments. They mentioned that the absence of $m^5C$ modification alters the translation quality, thereby induces the lifespan extension. Considering that the $m^1A$ modification of rRNA in yeast and mammal is involved in the ribosome formation (6, 95), I propose a possible mechanism that the RRAM-1-mediated change of translation contributes to the lifespan regulation.

Importantly, I found that RRAM-1 and NML could be related to the regulation of autophagy in my study. Western blotting experiments revealed that the reduction of RRAM-1 and NML increased the lipidated forms of LGG-1 and LC3-II, respectively. Until now, there have been many evidences that autophagy plays a key role in lifespan regulation (9-12). Therefore, my observations about the autophagic phenotype induced by RRAM-1 down-regulation suggest that autophagy links the rRNA $m^1A$ modification

to the regulation of lifespan.

# Chapter IV.

## Concluding Remarks

RNAs, including mRNA, tRNA and rRNA, play fundamental roles in gene transduction processes. These RNAs are modified post-transcriptionally in all three domains of life (Archaea, Bacteria, and Eukaryota). There are over 100 different chemical types of RNA modifications (1). Although roles for DNA and protein modifications in the regulation of gene expression are well-established, much less is understood about how RNA modifications modulate RNA functions and affect diverse biological phenomena.

Among the known RNA modifications, the $m^1A$ modification, one of the base methylations, has been identified in all three major RNA species (mRNA, tRNA, and rRNA). Extensive enzymological and functional analyses have been conducted in tRNAs (3-5, 108). In contrast, the responsible methyltransferases and the physiological functions of the rRNA $m^1A$ modification, especially in multicellular organisms, are largely unknown.

Remarkably, in a recent report, yeast Rrp8 has been identified as the first methyltransferase responsible for the $m^1A$ modification of yeast 25S rRNA (6). Thus, in chapter II, I focused on mammalian NML, which is a homolog of yeast Rrp8, and demonstrated that NML is required for the $m^1A$ modification of human and mouse 28S

rRNA, which corresponds with yeast 25S rRNA. Furthermore, I revealed that NML contributes to formation of the 60S ribosomal subunit. Considering that 28S rRNA is a major component of the 60S ribosomal subunit, the NML-mediated $m^1A$ modification may be important for maintaining its conformation. Importantly, depleting NML suppresses cell proliferation in a p53-dependent manner. These results suggest a novel role of rRNA $m^1A$ modification in mammal, which links ribosome biogenesis to the p53-mediated regulation of cell proliferation.

RNA methylations are regulated not only by methyltransferases but also by demethylases (82-85). In the case of the $m^1A$ modification, $m^1A$ demethylases were identified in mammalian mRNA and tRNA within the past decade (91-94). On the other hand, it is totally unknown whether the rRNA $m^1A$ modification is reversible. Further studies are needed, and the unraveling of this point would promote our grasp of RNA modification dynamics.

Previously, the *in vivo* function of the rRNA $m^1A$ modification was largely unknown. In chapter III, to address this issue, I examined the function of T07A9.8 (RRAM-1), which is the *C. elegans* homolog of human NML. From these investigations, I identified the existence of an $m^1A$ modification in *C. elegans* 26S rRNA for the first time and demonstrated that RRAM-1 is responsible for this

modification. Moreover, I found that RRAM-1 is involved in regulating autophagy and lifespan. Intriguingly, it has been considered that autophagy plays a key role in longevity (9-12). In conclusion, these novel discoveries suggest that the rRNA $m^1A$ modification links autophagy to the regulation of lifespan in multicellular organisms.

## Acknowledgments

I would like to express my gratitude to all those who provided me direction, support, and encouragement during the preparation of this dissertation. I especially wish to appreciate Professor Akiyoshi Fukamizu for all his kind guidance and support throughout my research work. I am indebted to Dr. Keiko Hirota, Dr. Koichiro Kako, Professor Keiji Tanimoto, Associate Professor Keiji Kimura, Dr. Yuka Nakajima, Dr. Tsuyoshi Waku, Mr. Sho Araoi, Ms. Wan Huahua, Mr. Naoaki Sumi, Ms. Mai Miyata and Mr. Naoto Nomura for their teaching about the fruitful discussions or experimental techniques. I am also grateful to Professor Akira Kobayashi and Professor Toshiyuki Shimizu for the experimental advice.

Finally, I greatly appreciate the helps of my parents and friends.

The chapter II and III is based in part on the following published papers, respectively.

Chapter II;

Waku, T., Nakajima, Y., Yokoyama, W., Nomura, N., Kako, K., Kobayashi, A., Shimizu, T., Fukamizu, A. (2016) NML-mediated rRNA base methylation links ribosomal subunit formation to cell proliferation in a p53-dependent manner. *Journal of Cell Science*, **129**, 2382-2393

Chapter III;

Yokoyama, W., Hirota, K., Wan, H., Sumi, N., Miyata, M., Araoi, S., Nomura, N., Kako, K., Fukamizu, A. (2017) rRNA adenine methylation requires *T07A9.8* gene as *rram-1* in *Caenorhabditis elegans*. *Journal of Biochemistry*, accepted.

## References


1. Machnicka, M.A., Milanowska, K., Osman Oqlou, O., Purta, E., Kurkowska, M., Olchowik, A., Januszewski, W., Kalinowski, S., Dunin-Horkawicz, S., Rother, K. M., Helm, M., Bujnicki, J.M., Grosjean, H. (2013) MODOMICS: a database of RNA modification pathway—2013 update. *Nuleic Acids Res.* **41**, D262-267.
2. Dunn, D. B. (1961) The occurrence of 1-methyladenosine in ribonucleic acid. *Biochim. Biophys. Acta.*, **46**, 198-200.
3. Oerum, S., Dégut, C., Barraud, P., Tisné, C. (2017) $m^1A$ Post-Transcriptional Modification in tRNAs. *Biomolecules* **7**, E20.
4. Anderson, J., Phan, L., Cuesta, R., Carlson, B.A., Pak, M., Asano, K., Björk, G.R., Tamame, M., Hinnebusch, A.G. (1998) The essential Gcd10p-Gcd14p nuclear complex is required for 1-methyladenosine modification and maturation of initiator methionyl-tRNA. *Genes Dev.*, **12**, 3650-3662.
5. Ozanick, S., Krecic, A., Andersland, J., Anderson, J.T. (2005) The bipartite structure of the tRNA m1A58 methyltransferase from *S. cerevisiae* is conserved in humans. *RNA*, **11**, 1281-1290.
6. Peifer, C., Sharma, S., Watzinger, P., Lamberth, S., Kötter, P., Entian, K.D. (2013) Yeast Rrp8p, a novel methyltransferase responsible for $m^1A$ 645 base modification

of 25S rRNA. *Nucleic Acids Res.* **41**, 1151-1163.

7. Thumel, C.S. (2001) Molecular mechanisms of developmental timing in *C. elegans* and *Drosophila*. *Dev. Cell*, **1**, 453-465.
8. Kenyon, C.J. (2010) The genetics of aging. *Nature*, **464**, 504-512.
9. Hars, E.S., Qi, H., Ryazanov, A.G., Jin, S., Cai, L., Hu, C., Liu, L.F. (2007) Autophagy regulates ageing in *C. elegans*. *Autophagy* **3**, 93-95.
10. Meléndez, A., Levine, B. (2009) Autophagy in *C. elegans*. *WormBook*, 1-26.
11. Rubinsztein, D.C., Mariño, G., Kroemer, G. (2011) Autophagy and aging. *Cell* **146**, 682-695.
12. Gelino, S., and Hansen, M. (2012) Autophagy – An Emerging Anti-Aging Mechanism. *J. Clin. Exp. Pathol.* **S4**, 006.
13. Nissen, P., Hansen, J., Ban, N., Moore, P.B., Steitz, T.A. (2000) The structural basis of ribosome activity in peptide bond synthesis. *Science* **289**, 920-930.
14. Steitz, T.A. and Moore, P.B. (2003) RNA, the first macromolecular catalyst: the ribosome is a ribozyme. *Trends Biochem. Sci.* **28**, 411-418.
15. Henras, A.K., Plisson-Chastang, C., O'Donohue, M.F., Chakraborty, A., Gleizes, P.E. (2015) An overview of pre-ribosomal RNA processing in eukaryotes. *Wiley Interdiscip. Rev.* **RNA** 6, 225-242.

16. Decatur, W.A. and Fournier, M.J. (2002) rRNA modifications and ribosome function. *Trends Biochem. Sci.* **27**, 344-351.

17. Hauenschild, R., Tserovski, L., Schmid, K., Thuring, K., Winz, M.L., Sharma, S., Entian, K.D., Wacheul, L., Lafontaine, D.L., Anderson, J., Alfonzo, J., Hidebrandt, A., Jäschke, A., Motorin, Y., Helm, M. (2015) The reverse transcription signature of N-1-methyladenosine in RNA-Seq is sequence dependent. *Nucleic Acids Res.* **43**, 9950–9964.

18. Sharma, S., and Lafontaine, D.L. (2015) 'View From A Bridge': A New Perspective on Eukaryotic rRNA Base Modification. *Trends Biochem. Sci.* **40**, 560-575.

19. Ishitani, R., Yokoyama, S. and Nureki, O. (2008) Structure, dynamics, and function of RNA modification enzymes. *Curr. Opin. Struct. Biol.* **18**, 330-339.

20. Gigova, A., Duggimpudi, S., Pollex, T., Schaefer, M., Koš, M. (2014) A cluster of methylations in the domain IV of 25S rRNA is required for ribosome stability. *RNA* **20**, 1632-1644.

21. Sharma, S., Watzinger, P., Kotter, P. and Entian, K.D. (2013) Identification of a novel methyltransferase, Bmt2, responsible for the N-1-methyl-adenosine base modification of 25S rRNA in *Saccharomyces cerevisiae*. *Nucleic Acids Res.* **41**, 5428-5443.

22. White, J., Li, Z., Sardana, R., Bujnicki, J.M., Marcotte, E.M., Johnson, A.W. (2008) Bud23 methylates G1575 of 18S rRNA and is required for efficient nuclear export of pre-40S subunits. *Mol. Cell Biol.* **28**, 3151-3161.

23. Schosserer, M., Minois, N., Angerer, T.B., Amring, M., Dellago, H., Harreither, E., Calle-Perez, A., Pircher, A., Peter Gerstl, M., Pfeifenberger, S., Brandl, C., Sonntagbauer, M., Kriegner, A., Linder, A., Weinhäusel, A., Mohr, T., Steiger, M., Mattanovich, D., Rinnerthaler, M., Karl, T., Sharma, S., Entian, K. D., Koš, M., Breitenbach, M., Wilson, I.B., Polacek, N., Grillari-Voglauer, R., Breitenbach-Koller, L., Grillari, J. (2016) Methylation of ribosomal RNA by NSUN5 is a conserved mechanism modulating organismal lifespan. *Nat. Commun.* **7**, 11530.

24. Haag, S., Kretschmer, J., and Bohnsack, M.T. (2015) WBSCR22/Merm1 is required for late nuclear pre-ribosomal RNA processing and mediates N7-methylation of G1639 in human 18S rRNA. *RNA* **21**, 180-187.

25. Anger, A.M., Armache, J.P., Berninghausen, O., Habeck, M., Subklewe, M., Wilson, D.N., Beckmann, R. (2013) Structures of the human and Drosophila 80S ribosome. *Nature* **497**, 80-85.

26. Khatter, H., Myasnikov, A.G., Natchiar, S.K. and Klaholz, B.P. (2015) Structure of the human 80S ribosome. *Nature* **520**, 640-645.

27. Fumagalli, S., Di Cara, A., Neb-Gulati, A., Natt, F., Schwemberger, S., Hall, J., Babcock, G.F., Bernardi, R., Pandolfi, P.P., Thomas, G. (2009) Absence of nucleolar disruption after impairment of 40S ribosome biogenesis reveals an rpL11-translation-dependent mechanism of p53 induction. *Nat. Cell Biol.* **11**, 501-508.

28. Sloan, K.E., Bohnsack, M.T. and Watkins, N.J. (2013) The 5S RNP couples p53 homeostasis to ribosome biogenesis and nucleolar stress. *Cell Rep.* **5**, 237-247.

29. Sulic, S., Panic, L., Barkic, M., Mercep, M., Uzelac, M., and Volarevic, S. (2005) Inactivation of S6 ribosomal protein gene in T lymphocytes activates a p53-dependent checkpoint response. *Genes Dev.* **19**, 3070-3082.

30. Bieging, K.T., Mello, S.S. and Attardi, L.D. (2014) Unravelling mechanisms of p53-mediated tumour suppression. *Nat. Rev. Cancer* **14**, 359-370.

31. Brooks, C.L. and Gu, W. (2010) New insights into p53 activation. *Cell Res.* **20**, 614-621.

32. Vousden, K.H. (2000) p53: death star. *Cell* **103**, 691-694.

33. Barna, M., Pusic, A., Zollo, O., Costa, M., Kondrashov, N., Rego, E., Rao, P.H., Ruggero, D. (2008) Suppression of Myc oncogenic activity by ribosomal protein haploinsufficiency. *Nature* **456**, 971-975.

34. Belin, S., Beghin, A., Solano-Gonzàlez, E., Bezin, L., Brunet-Manquat, S., Textoris,

J., Prats, A.C., Mertani, H.C., Dumontet, C., Diaz, J.J. (2009) Dysregulation of ribosome biogenesis and translational capacity is associated with tumor progression of human breast cancer cells. *PLoS One* **4**, e7147.

35. Belin, S., Kindbeiter, K., Hacot, S., Albaret, M.A., Roca-Martinez, J.X., Therizols, G., Grosso, O., Diaz, J.J. (2010) Uncoupling ribosome biogenesis regulation from RNA polymerase I activity during herpes simplex virus type 1 infection. *RNA* **16**, 131-140.
36. Figueiredo, V.C., Caldow, M.K., Massie, V., Markworth, J.F., Cameron-Smith, D., Blazevich, A.J. (2015) Ribosome biogenesis adaptation in resistance training-induced human skeletal muscle hypertrophy. *Am. J. Physiol. Endocrinol. Metab.* **309**, E72-83.
37. Marcel, V., Ghayad, S.E., Belin, S., Therizols, G., Morel, A.P., Solano-Gonzalez, E., Vendrell, J.A., Hacot, S., Mertani, H.C., Albaret, M.A., Boutdon, J.C., Jordan, L., Thompson, A., Tafer, Y., Cong, R., Bouvet, P., Saurin, J.C., Catez, F., Prats, A.C, Puisieux, A., Diaz, J.J. (2013) p53 acts as a safeguard of translational control by regulating fibrillarin and rRNA methylation in cancer. *Cancer Cell* **24**, 318-330.
38. Grummt, I. and Ladurner, A.G. (2008) A metabolic throttle regulates the epigenetic state of rDNA. *Cell* **133**, 577-580.

39. Murayama, A., Ohmori, K., Fujimura, A., Minami, H., Yasuzawa-Tanaka, K., Kuroda, T., Oie, S., Daitoku, H., Okuwaki, M., Nagata, K., Fukamizu, A., Kimura, K., Shimizu, T., Yanagisawa, J. (2008) Epigenetic control of rDNA loci in response to intracellular energy status. *Cell* **133**, 627-639

40. Oie, S., Matsuzaki, K., Yokoyama, W., Tokunaga, S., Waku, T., Han, S.I., Iwasaki, N., Mikogai, A., Yasuzawa-Tanaka, K., Kishimoto, H., Hiyoshi, H., Nakajima, Y., Araki, T., Kimura, K., Yanagisawa, J., Murayama, A. (2014) Hepatic rRNA transcription regulates high-fat-diet-induced obesity. *Cell Rep.* **7**, 807-820

41. Bunz, F., Dutriaux, A., Lengauer, C., Waldman, T., Zhou, S., Brown, J.P., Sedivy, J.M., Kinzler, K.W., and Vogelstein, B. (1998) Requirement for p53 and p21 to sustain G2 arrest after DNA damage. *Science* **282**, 1497-1501.

42. Lin, J., Lai, S., Jia, R., Xu, A., Zhang, L., Lu, J. and Ye, K. (2011) Structural basis for site-specific ribose methylation by box C/D RNA protein complexes. *Nature* **469**, 559-563.

43. Dignam, J.D., Lebovitz, R.M., and Roeder, R.G. (1983) Accurate transcription initiation by RNA polymerase II in a soluble extract from isolated mammalian nuclei. *Nucleic Acids Res.* **11**, 1475-1489.

44. Cozen, A.E., Quartley, E., Holmes, A.D., Hrabeta-Robinson, E., Phizicky, E.M.,

and Lowe, T.M. (2015) ARM-seq: AlkB-facilitated RNA methylation sequencing reveals a complex landscape of modified tRNA fragments. *Nat. Methods* **12**, 879-884.

45. Crain, P.F. (1990) Preparation and enzymatic hydrolysis of DNA and RNA for mass spectrometry. *Methods Enzymol.* **193**, 782-790.

46. Al-Jubran, K., Wen, J., Abdullahi, A., Roy Chaudhury, S., Li, M., Ramanathan, P., Matina, A., De, S., Piechocki, K., Rugjee, K.N., Brogna, S. (2013) Visualization of the joining of ribosomal subunits reveals the presence of 80S ribosomes in the nucleus. *RNA* **19**, 1669-1683.

47. Shyu, Y.J., Suarez, C.D., Hu, C.D. (2008) Visualization of ternary complexes in living cells by using a BiFC-based FRET assay. *Nat. Protoc.* **3**, 1693-1702.

48. Hu, C.D., Chinenov, Y. and Kerppola, T.K. (2002) Visualization of interactions among bZIP and Rel family proteins in living cells using bimolecular fluorescence complementation. *Mol. Cell* **9**, 789-798.

49. Tuorto, F., Liebers, R., Musch, T., Schaefer, M., Hofmann, S., Kellner, S., Frye, M., Helm, M., Stoecklin, G., Lyko, F. (2012) RNA cytosine methylation by Dnmt2 and NSun2 promotes tRNA stability and protein synthesis. *Nat. Struct. Mol. Biol.* **19**, 900-905.

50. Lee, M.S., Kim, B., Oh, G.T., Kim, Y.J. (2013) OASL1 inhibits translation of the type I interferon-regulating transcription factor IRF7. *Nat. Immunol.* **14**, 346-355.

51. Morello, L.G., Hesling, C., Coltri, P.P., Castilho, B.A., Rimokh, R. and Zanchin, N.I. (2011) The NIP7 protein is required for accurate pre-rRNA processing in human cells. *Nucleic Acids Res.* **39**, 648-665.

52. Itani, O.A., Cornish, K.L., Liu, K.Z., Thomas, C.P. (2003) Cycloheximide increases glucocorticoid-stimulated alpha -ENaC mRNA in collecting duct cells by p38 MAPK-dependent pathway. *Am. J. Physiol. Renal Physiol.* **284**, F778-787.

53. Mieulet, V., Roceri, M., Espeillac, C., Sotiropoulos, A., Ohanna, M., Oorschot, V., Klumperman, J., Sandri, M., Pende, M. (2007) S6 kinase inactivation impairs growth and translational target phosphorylation in muscle cells maintaining proper regulation of protein turnover. *Am. J. Physiol. Cell Physiol.* **293**, C712-722.

54. Clèries, R., Galvez, J., Espino, M., Ribes, J., Nunes, V., de Heredia, M.L. (2012) BootstRatio: A web-based statistical analysis of fold-change in qPCR and RT-qPCR data using resampling methods. *Comput. Biol. Med.* **42**, 438-445.

55. Schapira, M. (2016) Structural Chemistry of Human RNA Methyltransferases. *ACS Chem. Biol.* **11**, 575-582

56. Yang, L., Song, T., Chen, L., Kabra, N., Zheng, H., Koomen, J., Seto, E., Chen, J.

(2013) Regulation of SirT1-nucleomethylin binding by rRNA coordinates ribosome biogenesis with nutrient availability. *Mol. Cell. Biol.* **33**, 3835-3848.

57. Bousquet-Antonelli, C., Vanrobays, E., Gélugne, J.P., Caizergues-Ferrer, M., Henry, Y. (2000) Rrp8p is a yeast nucleolar protein functionally linked to Gar1p and involved in pre-rRNA cleavage at site A2. *RNA* **6**, 826-843.

58. Lapeyre, B. (2005) Conserved ribosomal RNA modification and their putative roles in ribosome biogenesis and translation. *Topics in Curr. Genet.* **12**, 263-284

59. Baxter-Roshek, J.L., Petrov, A.N., Dinman, J.D. (2007) Optimization of ribosome structure and function by rRNA base modification. *PLoS One* **2**, e174

60. Polikanov, Y.S., Melnikov, S.V., Söll, D. and Steitz, T.A. (2015) Structural insights into the role of rRNA modifications in protein synthesis and ribosome assembly. *Nat. Struct. Mol. Biol.* **22**, 342-344.

61. Blobel, G., and Sabatini, D. (1971) Dissociation of mammalian polyribosomes into subunits by puromycin. *Proc. Natl. Acad. Sci. U. S. A.* **68**, 390-394.

62. Miliani de Marval, P.L. and Zhang, Y. (2011) The RP-Mdm2-p53 pathway and tumorigenesis. *Oncotarget* **2**, 234-238.

63. Zhang, Y. and Lu, H. (2009) Signaling to p53: ribosomal proteins find their way. *Cancer Cell* **16**, 369-377.

64. Russo, A., Russo, G. (2017) Ribosomal proteins control or bypass p53 during nucleolar stress. *Int. J. Mol. Sci.* **18**, 140.

65. Deisenroth, C. and Zhang, Y. (2010) Ribosome biogenesis surveillance: probing the ribosomal protein-Mdm2-p53 pathway. *Oncogene* **29**, 4253-4260.

66. Lohrum, M.A., Ludwig, R.L., Kubbutat, M.H., Hanlon, M., Vousden, K.H. (2003). Regulation of HDM2 activity by the ribosomal protein L11. *Cancer Cell* **3**, 577-587.

67. Zhang, Y., Wolf, G.W., Bhat, K., Jin, A., Allio, T., Burkhart, W.A. and Xiong, Y. (2003) Ribosomal protein L11 negatively regulates oncoprotein MDM2 and mediates a p53-dependent ribosomal-stress checkpoint pathway. *Mol. Cell. Biol.* **23**, 8902-8912.

68. Hoppe-Seyler, F., and Butz, K. (1993) Repression of endogenous p53 transactivation function in HeLa cervical carcinoma cells by human papillomavirus type 16 E6, human mdm-2, and mutant p53. *J. Virol.* **67**, 3111-3117.

69. Kierstead, T.D., and Tevethia, M.J. (1993) Association of p53 binding and immortalization of primary C57BL/6 mouse embryo fibroblasts by using simian virus 40 T-antigen mutants bearing internal overlapping deletion mutations. *J. Virol.* **67**, 1817-1829.

70. Tilleray, V., Constantinou, C., Clemens, M.J. (2006) Regulation of protein synthesis by inducible wild-type p53 in human lung carcinoma cells. *FEBS lett.* **580**, 1766-1770.

71. Song, T., Yang, L., Kabra, N., Chen, L., Koomen, J., Haura, E.B., Chen, J. (2013) The $NAD^+$ synthesis enzyme nicotinamide mononucleotide adenylyltransferase (NMNAT1) regulates ribosomal RNA transcription. *J. Biol. Chem.* **288**, 20908-20917.

72. Decatur, W.A. and Fournier, M.J. (2003) RNA-guided nucleotide modification of ribosomal and other RNAs. *J. Biol. Chem.* **278**, 695-698.

73. Koh, C.M., Iwata, T., Zheng, Q., Bethel, C., Yegnasubramanian, S., De Marzo, A.M. (2011) Myc enforces overexpression of EZH2 in early prostatic neoplasia via transcriptional and post-transcriptional mechanisms. *Oncotarget* **2**, 669-683.

74. Miller, D.M., Thomas, S.D., Islam, A., Muench, D., Sedoris, K. (2012) c-Myc and cancer metabolism. *Clin. Cancer Res.* **18**, 5546-5553.

75. Rodrigues-Corona, U., Sobol, M., Rodriguez-Zapata, L.C., Hopak, P., Castano, E. (2015) Fibrillarin from Archaea to human. *Biol. Cell* **107**, 159-174.

76. Itoh, K., Ishiwata, S., Ishida, N., Mizugaki, M. (1992) Diagnostic use of anti-modified nucleoside monoclonal antibody. *Tohoku J. Exp. Med.* **168**, 329-331.

77. Itoh, K., Mizugaki, M., Ishida, N. (1988) Preparation of a monoclonal antibody specific for 1-methyladenosine and its application for the detection of elevated levels of 1-methyladenosine in urines from cancer patients. *Jpn. J. Cancer Res.* **79**, 1130-1138.

78. Chow, C., Lamichhane, T.N., and Mahto, S.K. (2007) Expanding the nucleotide repertoire of the ribosome with post-transcriptional modifications. *ACS Chem. Biol.* **2**, 610-619.

79. Frye, M., Jaffrey, S.R., Pan, T., Rechavi, G., and Suzuki, T. (2016) RNA modifications: what have we learned and where are we headed? *Nat. Rev. Genet.* **17**, 365-372.

80. O'Connell, M. (2015) RNA modification and the epitranscriptome; the next frontier. *RNA* **21**, 703-704.

81. Liu, N., and Pan, T. (2015) RNA epigenetics. *Transl. Res.* **165**, 28-35.

82. Chan, C.T., Dyavaiah, M., DeMott, M.S., Taghizadeh, K., Dedon, P.C., Begley, T.J. (2010) A quantitative systems approach reveals dynamic control of tRNA modifications during cellular stress. *PLoS Genet.* **6**, e1001247.

83. Roundtree, I.A., Evans, M.E., Pan, T., He, C. (2017) Dynamic RNA Modifications in Gene Expression Regulation. *Cell* **169**, 1187-1200.

84. Wang, X., and He, C. (2014) Dynamic RNA modifications in posttranscriptional regulation. *Mol. Cell* **56**, 5-12.

85. Yi, C., and Pan, T. (2011) Cellular Dynamics of RNA Modification. *Acc. Chem. Res.* **44**, 1380-1388.

86. Motorin, Y., and Helm, M. (2011) RNA nucleotide methylation. *Wiley Interdiscip. Rev. RNA* **2**, 611-631.

87. Jonkhout, N., Tran, J., Smith M.A., Schonrock N., Mattick J.S., Novoa, E.M. (2017) The RNA modification landscape in human disease. *RNA* in press

88. Hall, R.H. (1963) Method for isolation of 2'-*O*- methylribonucleosides and $N^1$-methyladenosine from ribonucleic acid. *Biochim. Biophys. Acta* **68**, 278-283.

89. Iwanami, Y., and Brown, G.M. (1968) Methylated bases of ribosomal ribonucleic acid from HeLa cells. *Arch. Biochem. Biophys.* **126**, 8-15.

90. Song, J., and Yi, C. (2017) Chemical Modifications to RNA: A New Layer of Gene Expression Regulation. *ACS Chem. Biol.* **12**, 316-325.

91. Dominissini, D., Nachtergaele, S., Moshitch-Moshkovitz, S., Peer, E., Kol, N., Ben-Haim, M.S., Dai, Q., Di Segni, A., Salmon-Divon, M., Clark, W.C., Zheng, G., Pan, T., Solomon, O., Eyal, E., Hershkovitz, V., Han, D., Doré, L.C., Amariglio, N., Rechavi, G., He, C. (2016) The dynamic $N^1$-methyladenosine methylome in

eukaryotic messenger RNA. *Nature* **530**, 441-446.

92. Ueda, Y., Ooshio, I., Fusamae, Y., Kitae, K., Kawaguchi, M., Jingushi, K., Hase, H., Harada, K., Hirata, K., Tsujikawa, K. (2017) AlkB homolog 3-mediated tRNA demethylation promotes protein synthesis in cancer cells. *Sci. Rep.* **7**, 42271.

93. Liu, F., Clark, W., Luo, G., Wang, X., Fu, Y., Wei, J., Wang, X., Hao, Z., Dai, Q., Zheng, G., Ma, H., Han, D., Evans, M., Klungland, A., Pan, T., He, C. (2016) ALKBH1-Mediated tRNA Demethylation Regulates Translation. *Cell* **167**, 816-828.

94. Li, X., Xiong, X., Wang, K., Wang, L., Shu, X., Ma, S., Yi, C. (2016) Transcriptome-wide mapping reveals reversible and dynamic $N^1$-methyladenosine methylome. *Nat. Chem. Biol.* **12**, 311-316.

95. Waku, T., Nakajima, Y., Yokoyama, W., Nomura, N., Kako, K., Kobayashi, A., Shimizu, T., Fukamizu, A. (2016) NML-mediated rRNA base methylation links ribosomal subunit formation to cell proliferation in a p53-dependent manner. *J. Cell Sci.* **129**, 2382-2393.

96. Kaletta, T., and Hengartner, M.O. (2006) Finding function in novel targets: *C. elegans* as a model organism. *Nat. Rev. Drug Discov.* **5**, 386-398.

97. Shaye, D.D., and Greenwald, I. (2011) OrthoList: a compendium of *C. elegans*

genes with human orthologs. *PLoS One* **6**, e20085.

98. Takahashi, Y., Daitoku, H., Hirota, K., Tamiya, H., Yokoyama, A., Kako, K., Nagashima, Y., Nakamura, A., Shimada, T., Watanabe, S., Yamagata, K., Yasuda, K., Ishii, N., Fukamizu, A. (2011) Asymmetric arginine dimethylation determines life span in *C. elegans* by regulating forkhead transcription factor DAF-16. *Cell Metab.* **13**, 505-516.

99. Hirota, K., Shigekawa, C., Araoi, S., Sha, L., Inagawa, T., Kanou, A., Kako, K., Daitoku, H., Fukamizu, A. (2017) Simultaneous ablation of *prmt-1* and *prmt-5* abolishes asymmetric and symmetric arginine dimethylations in *Caenorhabditis elegans*. *J Biochem.* **161**, 521-527.

100. Higa, S., Maeda, N., Kenmochi, N., Tanaka, T. (2002) Location of 2'-*O*-methyl nucleotides in 26S rRNA and methylation guide snoRNAs in *C elegans*. *Biochem. Biophys. Res. Commun.* **297**, 1344-1349.

101. Hamilton, B., Dong, Y., Shindo, M., Liu, W., Odell, I., Ruvkun, G., Lee, S.S. (2005) A systematic RNAi screen for longevity genes in *C. elegans*. *Genes Dev.* **19**, 1544-1555.

102. Curran, S.P., and Ruvkun, G. (2007) Lifespan regulation by evolutionarily conserved genes essential for viability. *PLoS Genet.* **3**, e56.

103. Booth, L.N., and Brunet, A. (2016) The Aging Epigenome. *Mol. Cell.* **62**, 728-744.

104. Pan, H., and Finkel, T. (2017) Key proteins and pathways that regulate lifespan. *J. Biol. Chem.* **292**, 6452-6460.

105. Zhang, H., Chang, J.T., Guo, B., Hansen, M., Jia, K., Kovács, A. L., Kumsta, C., Lapierre, L.R., Legouis, R., Lin, L., Lu, Q., Meléndez, A., O'Rourke, E.J., Sato, K., Sato, M., Wang, X., Wu, F. (2015) Guidelines for monitoring autophagy in *Caenorhabditis elegans*. *Autophagy* **11**, 9-27.

106. Chen, Y., Scarcelli, V., Legouis, R. (2017) Approaches for Studying Autophagy in *Caenorhabditis elegans*. *Cells* **6**, E27.

107. Dong, Z.W., Shao, P., Diao, L.T., Zhou, H., Yu, C.H., Qu, L.H. (2012) RTL-P: a sensitive approach for detecting sites of 2'-*O*-methylation in RNA molecules. *Nucleic Acids Res.* **40**, e157

108. Macari, F., El-Houfi, Y., Boldina, G., Xu, H., Khoury-Hanna, S., Ollier, J., Yazdani, L., Zheng, G., Bièche, I., Legrand, N., Paulet, D., Durrieu, S., Byström, A., Delbecq, S., Lapeyre, B., Bauchet, L., Pannequin, J., Hollande, F., Pan, T., Teichmann, M., Vagner, S., David, A., Choquet, A., Joubert, D. (2016) TRM6/61 connects PKCα with translational control through tRNAi (Met) stabilization: impact on tumorigenesis. *Oncogene* **35**, 1785-1796.